Quantifying Entanglement in the One-Dimensional Heisenberg Spin Chain

by

© **Pouria Mirsadegh**

A thesis submitted to the School of Graduate Studies in partial fulfillment of the requirements for the degree of Master of Science.

Department of Physics and Physical Oceanography

Memorial University

May 2023

St. John's, Newfoundland and Labrador, Canada

Abstract

This thesis aims to investigate the entanglement properties of the one-dimensional Heisenberg spin chain, with a focus on the entanglement between pairs of spins. Specifically, we explore how entanglement depends on temperature and coupling constants without an external magnetic field and then consider the effect of an external magnetic field on entanglement.

To model the system, we utilize the Hamiltonian of the 1D Heisenberg spin chain and calculate the density matrix. We use the concurrence as a measure of entanglement, which is applicable to mixed state densities.

Our main findings demonstrate that the entanglement between pairs of spins in the Heisenberg spin chain increases as temperature decreases or coupling constants increase. We also identify a critical range of magnetic fields in which the entanglement between spin pairs undergoes significant changes. Finally, we examine the relationship between entanglement and the number of lattice sites separating given pairs of spins. Our results reveal that as the number of lattice sites between pairs of spins increases, the entanglement between them decreases.

Overall, this study provides insights into the entanglement properties of the one-dimensional Heisenberg spin chain and sheds light on the factors that influence entanglement in quantum systems. These findings potentially have important implications for the design and development of quantum information processing devices.

Acknowledgements

I would like to express my deepest gratitude and appreciation to my supervisors, Dr. Stephanie H. Curnoe and Dr. James P. F. LeBlanc, for their invaluable guidance and support throughout this project. Their expertise, insightful comments, and constructive feedback have been instrumental in shaping my research and improving my academic skills. I am extremely grateful for the opportunity to work with such outstanding researchers and mentors.

I am also grateful to the Department of Physics and Physical Oceanography and the School of Graduate Studies at the Memorial University of Newfoundland for providing financial support for this project. Without their support, this research would not have been possible.

Finally, I would like to extend a heartfelt thank you to my parents for their unwavering love, encouragement, and support throughout my academic journey. Their sacrifices, belief in me, and constant motivation have been my source of strength and inspiration. I am truly blessed to have them in my life.

Table of contents

List of figures

List of symbols

σ_i	Pauli matrices
S_i	Spin operators
H	Hamiltonian
J_i	Coupling constants
$\hbar$	Dirac constant $= 6.582 \times 10^{-16} eV.s$
ρ	Density matrix
ρ_{ij}	Reduced density matrix
Z	Partition function
C	Concurrence
N	Negativity
E_f	Entanglement of formation
B	Magnetic field
E_N	Logarithmic Negativity
λ_i	Energy eigenvalues
k_B	Boltzmann constant

List of abbreviations

1D	One dimensional
EPR	Einstein–Podolsky–Rosen
PPT	Positive partial transpose

Chapter 1

Introduction

1.1 Quantum Entanglement

Entanglement is a quantum phenomenon in which the measurement of the quantum state of one part of a system depends on the results of measurements performed on the other parts, no matter how far apart they are in space [1] [2] [3]. As a result, observation of one of the entangled parts will automatically provide information about the state of the other parts, irrespective of the distance between them. Furthermore, any action to one of these parts will invariably impact the others in the entangled system [4]. Entanglement is a quantum mechanical feature, which is impossible to describe in classical physics [5].

Entanglement has been found to play a critical role in quantum information processing and quantum computing. In quantum computing, entanglement is the key resource that enables exponential speedup in certain computational tasks, such as factorization and searching algorithms [5]. Moreover, entanglement is also essential for error correction and fault-tolerance in quantum computing architectures. Another important application of entanglement is quantum teleportation, which is the transfer of quantum information from one location to another without physically moving the information carrier. Entanglement is used to "teleport" the quantum state of one particle onto another, allowing for the transfer of information with perfect fidelity [1].

In addition to its applications in quantum information processing and quantum computing, quantum entanglement plays a critical role in condensed matter physics,

where it is used to describe materials with strong correlations between particles. In particular, the detection and classification of topological phases of matter can be achieved through the use of entanglement-based measures, such as the entanglement entropy, which provide a powerful tool for characterizing the quantum properties of these materials. The connection between entanglement and topological phases of matter was first established by Levin and Wen in their seminal paper on detecting topological order in ground state wave functions [6]. Since then, entanglement has become a crucial tool for understanding and characterizing the properties of a wide variety of topological materials, including topological insulators [7] and topological superconductors [8], materials which have the potential for new technological applications, such as topological quantum computing.

An example of entanglement in quantum systems can involve the spin of two electrons. Electrons have a fundamental property called spin, which is a quantum mechanical angular momentum. Unlike classical angular momentum, the spin of an electron can only take on certain discrete values, typically referred to as "up" and "down". However, because of the principles of quantum mechanics, the spin of electrons is inherently uncertain, meaning that prior to measurement, we do not know with certainty which of the possible spin states an electron is in. It is through this inherent uncertainty that the phenomenon of entanglement arises between two or more quantum systems. If the electrons are entangled, then those two spins are correlated such that if one of the electrons is measured to be spin up, then the other must have spin down. This power of prediction of quantum mechanics refers to quantum entanglement.

In 1935, Albert Einstein raised concerns about the predictions of quantum mechanics regarding the behavior of entangled particles [9]. The prediction of quantum mechanics refers to the ability of quantum mechanics to make probabilistic predictions about the behavior of quantum systems. For example, one such prediction is the expected correlation between measurements made on two separated entangled particles. Suppose we send two entangled photons to two separate observers, Alice and Bob, on different sides of the world. As Niels Bohr said, while these two entangled photons are going outward, they do not have a fixed orientation of their spins [10]. All we know about them is that they are entangled. As a result, if Alice measures her electron with spin up, then Bob will have spin down. However, the electron's spin sent to Bob was not determined until Alice measured it. This situation is where

Einstein felt there was a problem with quantum entanglement because it seemed to indicate that the act of Alice measuring her electron spin affected the spin of Bob's electron. If Alice measures her electron spin up, then immediately, there will be some influence on Bob's electron spin to ensure his electron spin is down, even if they are light-years apart.

Einstein described this problem in quantum entanglement as "spooky action at a distance." In 1935, Albert Einstein and his colleagues Boris Podolsky and Nathan Rosen suggested that there has to be an alternative to this problem because spooky action at a distance should not be allowed in physics [9]. Einstein showed that no signal or information could be transmitted faster than light. Therefore, there has to be some time for a signal to span the distance, and we cannot have this instantaneous action at a distance [9]. This problem is also known as the Einstein–Podolsky–Rosen paradox (EPR paradox). Einstein suggested that there must be some property that we could not measure. He indicated that these two electrons had some property that somehow fixed their spins in advance. He called this property a "hidden variable" [9].

In 1964, John Stewart Bell [11] proved that quantum mechanics is incompatible with local hidden-variable theories. He showed that "If [a hidden-variable theory] is local it will not agree with quantum mechanics, and if it agrees with quantum mechanics it will not be local." [12] Bell's theorem provides a way to test the predictions of quantum mechanics against the classical physics. It is based on the concept of Bell inequalities, which are certain mathematical inequalities that are satisfied by any theory that assumes "local realism." Local realism is the idea that physical properties of objects exist independently of measurements, and that these properties are not influenced by the measurement of other distant objects. However, quantum mechanics predicts that certain measurements on entangled particles violate Bell inequalities, indicating that local realism is not a valid assumption. This violation is known as Bell's inequality violation, and it provides strong evidence for the non-local nature of entanglement [5]. For a more detailed discussion on the mathematical description of Bell's inequality, please refer to Appendix A.

1.2 Quantum Spin Systems

A quantum spin system is a set of interacting spins, for example, a spin chain consisting of N spins [13][14]. On each site of the spin chain, we consider a spin $\frac{1}{2}$ particle, such as an electron. In the quantum spin chain, every electron can be in a spin up or spin down state, and they are the basis of a two-dimensional Hilbert state for each electron in the chain [13].

As an example of a spin system, consider the maximally entangled state for the two-electron spin system:

$$|\psi_s\rangle = \frac{1}{\sqrt{2}}(|+-\rangle - |-+\rangle)$$

Where ψ_s is the singlet state. The electrons in this state are maximally entangled. In other words, the spin directions of two electrons are guaranteed to be opposite when measured. If the spin of one electron is up, the other one must be down.

1.3 Quantifying Entanglement

Quantifying entanglement refers to any scheme that assigns a quantitative value for entanglement in a two-part system, such that unentangled states have a value of zero and the entanglement of pure states monotonically increases to a maximum value for a singlet or similar state. Quantifying the amount of entanglement between particles is important for developing applications such as quantum computing and cryptography [1][15][16].

In this section, we briefly describe a scheme to quantify entanglement for pure states. We can start with a general pure state for two spins like:

$$|\psi\rangle = C_{++}|++\rangle + C_{+-}|+-\rangle + C_{-+}|-+\rangle + C_{--}|--\rangle, \tag{1.1}$$

with

$$|C_{++}|^2 + |C_{+-}|^2 + |C_{-+}|^2 + |C_{--}|^2 = 1. \tag{1.2}$$

If a state can be expressed in a factorizable format, then it is not considered to be

entangled. This is because measurements performed on one subsystem have no effect on measurements performed on the other subsystem, indicating a lack of entanglement between the subsystems. In contrast, entangled states cannot be written in a factorizable format. A general unentangled state takes the form

$$(a_1|+\rangle + a_2|-\rangle) \otimes (b_1|+\rangle + b_2|-\rangle), \tag{1.3}$$

where $|a_1|^2+|a_2|^2 = |b_1|^2+|b_2|^2 = 1$. Therefore, if the state in Eq. 1.1 is not entangled, we have:

$$C_{++} = a_1 b_1 \ , \ C_{+-} = a_1 b_2 \ , \ C_{-+} = a_2 b_1 \ , \ C_{--} = a_2 b_2.$$

If we solve the equation for a_1, we can write:

$$a_1 = \frac{C_{++}}{b_1} = \frac{C_{++}a_2}{C_{-+}} = \frac{C_{++}C_{--}}{C_{-+}b_2} = \frac{C_{++}C_{--}}{C_{-+}C_{+-}}a_1. \tag{1.4}$$

We find that $\frac{C_{++}C_{--}}{C_{-+}C_{+-}} = 1$, in other words $C_{++}C_{--} - C_{-+}C_{+-} = 0$ for an unentagled state. However, for the singlet state, we have $C_{++}C_{--} - C_{-+}C_{+-} = \frac{1}{2}$ which is a maximum for this quantity subject to the constraint (1.2). Therefore, we can take $|C_{++}C_{--} - C_{-+}C_{+-}|$ as a measure of the entanglement of pure states. If this value is zero, the state is not entangled. If this value is non-zero, the state is entangled, and for $\frac{1}{2}$, the state is maximally entangled. The coefficient measure only works for quantifying the entanglement of pure states, and it is not possible to use this measure for mixed states.

1.4 Entanglement in Spin Systems

Entanglement is an important concept in the study of quantum spin systems, as it provides a way to understand the collective behavior of a large number of interacting spins. In particular, the entanglement properties of spin systems have been shown to have important implications for quantum phase transitions, where the system undergoes a change in its ground state as a parameter, such as a magnetic field, is varied [17][18]. One example of a spin system that has been extensively studied for its entanglement properties is the one-dimensional Heisenberg spin chain, which describes a

line of interacting spin $\frac{1}{2}$ particles. In this thesis, we study entanglement between each pair of spins for the one-dimensional Heisenberg spin chain in thermal equilibrium.

Previous studies have shown that the entanglement of a pair of spins in a one-dimensional Heisenberg spin chain depends on the temperature and the coupling constants, but these studies have typically focused on small spin chains or specific scenarios. Refs. [19][20] studied the entanglement of two spins in the Heisenberg spin chain versus the magnetic field and temperature, while Ref. [21] investigated the entanglement of three spins in a chain with an external magnetic field and different coupling constants. Moreover, Ref. [22] studied the entanglement of four spins in the Heisenberg spin chain. However, there has been relatively little research on how the entanglement of a pair of spins depends on the number of lattice sites separating given pairs of spins or how it changes for larger spin chains.

Our research addresses these gaps in the existing literature by studying the entanglement of a pair of spins in one-dimensional Heisenberg spin chains with up to 10 spins for various scenarios. Specifically, we investigate how the entanglement depends on the temperature and coupling constants with and without an external magnetic field and how it changes for the different number of lattice sites separating given pairs.

In conclusion, our research builds upon the existing literature by studying the entanglement of a pair of spins in one-dimensional Heisenberg spin chains with up to 10 spins for various scenarios. Our study fills an important gap in the existing literature and provides new insights into the behavior of entanglement in these systems. Furthermore, our results have potential applications in quantum information processing and quantum computing.

1.5 Outline

The remainder of the thesis is organized as follows. Chapter Two describes the mathematical tools for calculating entanglement, including the square root, natural logarithm, and exponential of a matrix, as well as measurements such as concurrence, entanglement entropy, entanglement of formation, and logarithmic negativity for quantifying entanglement in both pure and mixed states. In Chapter Three, the one-dimensional Heisenberg spin chain model is introduced and two entanglement measurements, concurrence and logarithmic negativity, are compared to determine

the most suitable method for this study. Chapter Four investigates the dependence of entanglement on coupling constants and temperature in the Heisenberg spin chain without a magnetic field, and then incorporates an external magnetic field for fixed values of these parameters. Additionally, the entanglement is calculated for different pairs of spins on the chain, such as nearest neighbors and next-nearest neighbors. Chapter Five provides an overview of the research findings, the significance of the results, and potential future research directions and applications. Finally, the Appendix includes computational codes used in the research and examples of mathematical tools employed in the calculations.

Chapter 2

Mathematical and Computational Tools

2.1 Introduction

This chapter serves as an introduction to the mathematical, quantum information, and computational tools that are utilized throughout this thesis. The goal is to provide the reader with a comprehensive understanding of these tools and how they are applied in studying the entanglement properties of the one-dimensional Heisenberg spin chain.

The chapter is organized as follows: In Section 2.2, we provide an overview of the basic mathematical tools necessary to describe the entanglement in spin systems, including the calculation of the density matrix from the Hamiltonian matrix. Section 2.3 provides a brief introduction to the quantum information tools used to quantify entanglement for both pure and mixed states, while Section 2.4 describes the computational tools utilized to compute entanglement in this thesis. By the end of this chapter, the reader will have a thorough understanding of the mathematical, quantum information, and computational tools utilized in this study.

2.2 Mathematical Tools

This section introduces the mathematical concepts and tools that are utilized in this thesis to study the entanglement properties of the one-dimensional Heisenberg spin

chain. We will cover important topics such as the Hamiltonian matrix, density matrix, natural logarithm of a matrix, exponential of a matrix, and the square root of a matrix.

These mathematical tools are essential for understanding the behavior of spin chains and for calculating the density matrix, which plays a crucial role in quantifying the entanglement between pairs of spins. By the end of this section, the reader will have a clear understanding of the mathematical tools utilized in this study and their significance in studying the entanglement properties of the one-dimensional Heisenberg spin chain.

2.2.1 Natural logarithm, Exponential, and Square root of a Matrix

This section explores some mathematical tools for matrices, such as the natural logarithm of a matrix, the exponential of a matrix, and the square root of a matrix, as we need these tools to calculate the concurrence.

For a diagonalizable matrix A, the natural logarithm of A is defined as follows [23]:

$$\log A = V(\log A^{'})V^{-1}. \tag{2.1}$$

Where V is a matrix of eigenvectors of A such that each of the elements in a column of V is the component of an eigenvector of A, and V^{-1} is the inverse matrix of V. $A^{'}$ is a diagonal matrix whose elements are the eigenvalues of A. By replacing the natural logarithm of each element of $A^{'}$, we can find the natural logarithm of matrix $A^{'}$ as it is a diagonal matrix and use equation (2.1) to find the natural logarithm of the matrix A.

The method to find the exponential of a matrix is very similar to the natural logarithm of a matrix, but we need to replace the exponential of each element of $A^{'}$ [24],

$$\exp A = V(\exp A^{'})V^{-1}. \tag{2.2}$$

It is worth noting that these formulas apply specifically to the natural logarithm and exponential functions, i.e., those with base e. This is because the eigenvectors and

eigenvalues of a matrix are typically complex, and the natural logarithm and exponential functions are well-defined for complex numbers. However, other logarithmic or exponential functions with different bases may not be well-defined for complex numbers, and therefore the above formulas may not apply in those cases.

2.2.2 Hamiltonian Matrix

The Hamiltonian matrix is a Hermitian matrix whose elements and dimensionality depend on the physics that governs the system [25]. For instance, the Hamiltonian of the Heisenberg spin chain has a dimension of 2^N where N is the number of spins. We can write the Hamiltonian of the 1D Heisenberg model as below [26][27][28][29]:

$$H = \sum_{i=1}^{N-1} J_x S_x^i S_x^{i+1} + J_y S_y^i S_y^{i+1} + J_z S_z^i S_z^{i+1} - \sum_{i=1}^{N} B S_z^i, \tag{2.3}$$

where J_i is the coupling constant at site i, S_i is the spin operator at site i, B is the external magnetic field, and N is the number of spins in the chain. For example, for a chain with three spins without the external magnetic field, the Hamiltonian matrix is:

$$H = \sum_{i=1}^{2} J_x S_x^i S_x^{i+1} + J_y S_y^i S_y^{i+1} + J_z S_z^i S_z^{i+1}, \tag{2.4}$$

which is an eight-by-eight square matrix where S_x, S_y, and S_z are the spin $\frac{1}{2}$ operators with matrices $\boldsymbol{S} = \frac{\hbar}{2}\boldsymbol{\sigma}$

$$\sigma_x = \begin{pmatrix} 0 & 1 \\ 1 & 0 \end{pmatrix}, \sigma_y = \begin{pmatrix} 0 & -i \\ i & 0 \end{pmatrix}, \sigma_z = \begin{pmatrix} 1 & 0 \\ 0 & -1 \end{pmatrix}.$$

These three matrices are known as Pauli matrices. Written explicitly as the tensor products of matrices, the Hamiltonian matrix is:

$$H = \frac{\hbar^2}{4}[J_x(\sigma_x^1 \otimes \sigma_x^2 \otimes \mathbf{I}) + J_y(\sigma_y^1 \otimes \sigma_y^2 \otimes \mathbf{I}) + J_z(\sigma_z^1 \otimes \sigma_z^2 \otimes \mathbf{I}) + J_x(\mathbf{I} \otimes \sigma_x^2 \otimes \sigma_x^3) + J_y(\mathbf{I} \otimes \sigma_y^2 \otimes \sigma_y^3) + J_z(\mathbf{I} \otimes \sigma_z^2 \otimes \sigma_z^3)].$$

Where I is the two by two identity matrix,

$$I = \begin{pmatrix} 1 & 0 \\ 0 & 1 \end{pmatrix}.$$

Thus the Hamiltonian matrix with three spins on the chain is

$$H = \frac{\hbar^2}{4} \begin{pmatrix} 2J_z & 0 & 0 & J_x - J_y & 0 & 0 & J_x - J_y & 0 \\ 0 & 0 & J_x + J_y & 0 & 0 & 0 & 0 & J_x - J_y \\ 0 & J_x + J_y & -2J_z & 0 & J_x + J_y & 0 & 0 & 0 \\ J_x - J_y & 0 & 0 & 0 & 0 & J_x + J_y & 0 & 0 \\ 0 & 0 & J_x + J_y & 0 & 0 & 0 & 0 & J_x - J_y \\ 0 & 0 & 0 & J_x + J_y & 0 & -2J_z & J_x + J_y & 0 \\ J_x - J_y & 0 & 0 & 0 & 0 & J_x + J_y & 0 & 0 \\ 0 & J_x - J_y & 0 & 0 & J_x - J_y & 0 & 0 & 2J_z \end{pmatrix}.$$

2.2.3 Density Matrix

In quantum mechanics, a density matrix describes the quantum state of a physical system. This section outlines some methods to find the density matrix for pure and mixed states [30]. To quantify entanglement, it is important to find the density matrix because it allows us to calculate the reduced density matrix, which describes the state of a subsystem of a larger quantum system. By analyzing the properties of the reduced density matrix, we can determine the degree of entanglement between the subsystems.

Pure States

A pure quantum state is a state that can be expressed as a singlet ket, which may be a linear combination of other kets [31]. For example, consider the pure state

$|\psi\rangle = \frac{1}{\sqrt{2}}(|+-\rangle + |-+\rangle)$, where the kets $|+\rangle$ and $|-\rangle$ are represented as column vectors and the states $|+-\rangle$ and $|-+\rangle$ are their tensor products.

$$|+\rangle = \begin{pmatrix}1\\0\end{pmatrix}, |-\rangle = \begin{pmatrix}0\\1\end{pmatrix},$$

$$|+-\rangle = \begin{pmatrix}1\\0\end{pmatrix} \otimes \begin{pmatrix}0\\1\end{pmatrix} = \begin{pmatrix}0\\1\\0\\0\end{pmatrix}, |-+\rangle = \begin{pmatrix}0\\1\end{pmatrix} \otimes \begin{pmatrix}1\\0\end{pmatrix} = \begin{pmatrix}0\\0\\1\\0\end{pmatrix}.$$

The density matrix for a pure state $|\psi\rangle$ can be defined as [30].

$$\rho = |\psi\rangle\langle\psi|, \tag{2.5}$$

where $\langle\psi|$ denotes the adjoint of the state vector $|\psi\rangle$. The density matrix operator is positive, semi-definite, Hermitian, and has trace one. The density matrix for the pure state $|\psi\rangle$ can be expressed as

$$\rho = \frac{1}{\sqrt{2}}(|+-\rangle + |-+\rangle) * \frac{1}{\sqrt{2}}(\langle+-| + \langle-+|)$$

$$= \frac{1}{2}(|+-\rangle\langle+-| + |+-\rangle\langle-+| + |-+\rangle\langle+-| + |-+\rangle\langle-+|).$$

Finally, the matrix form of the density matrix is

$$\rho = \frac{1}{\sqrt{2}}\begin{pmatrix}0\\1\\1\\0\end{pmatrix} \otimes \frac{1}{\sqrt{2}}\begin{pmatrix}0 & 1 & 1 & 0\end{pmatrix} = \frac{1}{2}\begin{pmatrix}0 & 0 & 0 & 0\\0 & 1 & 1 & 0\\0 & 1 & 1 & 0\\0 & 0 & 0 & 0\end{pmatrix}.$$

The density matrix of a pure state needs to satisfy some conditions. Firstly, it satisfies $\rho = \rho^2$:

$$\rho^2 = |\psi\rangle\langle\psi|\psi\rangle\langle\psi| = \rho. \tag{2.6}$$

Then the next condition is $Tr[\rho^2] = Tr[\rho] = 1$ for a pure state. The density matrix for the above pure state satisfies all the necessary conditions.

Mixed States and Hamiltonian

In the previous section, we discussed the calculation of the density matrix for a pure state. However, in many physical situations, we deal with mixed states. Therefore, it is essential to understand how to calculate the density matrix for a mixed state. In this section of the thesis, we will focus on the calculation of the density matrix for a mixed state. The density matrix for a mixed state is [5]:

$$\rho = \sum_j p_j |\psi_j\rangle\langle\psi_j|, \tag{2.7}$$

where $|\psi_j\rangle$ is a pure state with the probability p_j.

For a system in thermal equilibrium, the density matrix is given by [29]:

$$\rho = \frac{\exp(\frac{-H}{k_B T})}{Z}, \tag{2.8}$$

where k_B is the Boltzmann constant and $Z = Tr[\exp \frac{-H}{k_B T}]$ is the partition function. If the eigenstates of H are ψ_i with eigenvalues λ_i, $H|\psi_i\rangle = \lambda_i$ then

$$Z = \sum_i \exp \frac{-\lambda_i}{k_B T} \tag{2.9}$$

and

$$\rho = \frac{1}{Z} \sum_i \exp \frac{-\lambda_i}{k_B T} |\psi_i\rangle\langle\psi_i|. \tag{2.10}$$

For example, in the chain of three spins for $B = 0$ $J_x = J_y = J_z = 1$, the eigenvalues and eigenvectors of the Hamiltonian matrix are

$$\lambda_1 = \lambda_2 = -4, \lambda_3 = \lambda_4 = 0, \lambda_5 = \lambda_6 = \lambda_7 = \lambda_8 = 2$$

$$V_1 = |++\!+\rangle, V_2 = |--\!-\rangle,$$
$$V_3 = \frac{1}{\sqrt{2}}(|++\!-\rangle - |--\!+\rangle),$$
$$V_4 = \frac{1}{\sqrt{2}}(|-+\!-\rangle - |+-\!+\rangle),$$

$$V_5 = \frac{1}{\sqrt{3}}(|--+\rangle + |+-\rangle + |-+-\rangle),$$

$$V_6 = -\frac{1}{\sqrt{3}}(|++-\rangle + |+-+\rangle + |-++\rangle),$$

$$V_7 = \frac{1}{\sqrt{6}}(2|-+-\rangle - |--+\rangle - |+--\rangle),$$

$$V_8 = \frac{1}{\sqrt{6}}(2|+-+\rangle - |++-\rangle - |-++\rangle).$$

Now, we can utilize equation (2.8) to obtain the density matrix. As described in section 2.2.1, we can compute the exponential of a matrix using equation (2.2). By substituting the eigenvectors and eigenvalues of the Hamiltonian for $k_BT = 1$ in equation (2.2), we can determine the density matrix.

$$\rho = \begin{pmatrix} 0.0012 & 0 & 0 & 0 & 0 & 0 & 0 & 0 \\ 0 & 0.086 & -0.16 & 0 & 0.077 & 0 & 0 & 0 \\ 0 & -0.16 & 0.33 & 0 & -0.16 & 0 & 0 & 0 \\ 0 & 0 & 0 & 0.086 & 0 & -0.16 & 0.077 & 0 \\ 0 & 0.077 & -0.16 & 0 & 0.086 & 0 & 0 & 0 \\ 0 & 0 & 0 & -0.16 & 0 & 0.33 & -0.16 & 0 \\ 0 & 0 & 0 & 0.077 & & -0.16 & 0.086 & 0 \\ 0 & 0 & 0 & 0 & 0 & 0 & 0 & 0.0012 \end{pmatrix}.$$

2.2.4 Reduced Density Matrix

In order to quantify entanglement for a pair of spins in a one-dimensional Heisenberg spin chain, we need to calculate the reduced density matrix for that pair. The reduced density matrix captures the information about the entangled state of the pair, while ignoring the state of the other spins in the chain. This is necessary because the density matrix that we calculate based on the Hamiltonian matrix represents the entire chain of spins with an arbitrary number of spins in the chain, and it is not sufficient to determine the entanglement between a pair of spins.

The reduced density matrix was first introduced by Paul Dirac in 1930, and it is a fundamental tool in quantum mechanics for analyzing subsystems of a larger quantum system. By reducing the density matrix to the subsystem of interest, we can calculate entanglement measures such as the concurrence or negativity, which

quantify the degree of entanglement between pairs of spins in the chain [32].

Therefore, the introduction of the reduced density matrix is crucial for our analysis of entanglement in the one-dimensional Heisenberg spin chain, as it allows us to focus specifically on the entanglement between pairs of spins.

2.2.5 Partial Trace

To obtain the reduced density matrix of a pair of spins in the Heisenberg chain, we need to take the partial trace over all other spins in the chain. This process involves finding the trace of the density matrix over the degrees of freedom associated with the unwanted spins. For example, in the case of a three-spin Heisenberg chain, to calculate the reduced density matrix for spins one and two, we take the trace over the third spin. The resulting matrix is the reduced density matrix for spins one and two. The same procedure is repeated to find the reduced density matrix for other pairs of spins.

$$\rho_{1,2} = \sum_{\alpha=+-} \langle 3:\alpha|\rho|3:\alpha\rangle. \tag{2.11}$$

Using our example for ρ above, we can find the reduced density matrix for spin pairs one and two, two and three, and one and three as below:

$$\rho_{1-2} = \begin{pmatrix} 0.088 & 0 & 0 & 0 \\ 0 & 0.41 & -0.33 & 0 \\ 0 & -0.33 & 0.41 & 0 \\ 0 & 0 & 0 & 0.088 \end{pmatrix},$$

$$\rho_{2-3} = \begin{pmatrix} 0.088 & 0 & 0 & 0 \\ 0 & 0.41 & -0.33 & 0 \\ 0 & -0.33 & 0.41 & 0 \\ 0 & 0 & 0 & 0.088 \end{pmatrix},$$

$$\rho_{1-3} = \begin{pmatrix} 0.33 & 0 & 0 & 0 \\ 0 & 0.17 & 0.15 & 0 \\ 0 & 0.15 & 0.17 & 0 \\ 0 & 0 & 0 & 0.33 \end{pmatrix}.$$

As spins(1,2) and spins(2,3) are located on the edge of the spin chain, they have the same reduced density matrices. In the next chapter, we will use the reduced density matrix to calculate concurrence, which is a measure to quantify entanglement.

2.3 Quantum Information Tools

Entanglement is a fundamental concept in the field of quantum information, playing a vital role in various quantum applications such as quantum cryptography, quantum teleportation, and quantum computing. It arises from the non-local correlations between the components of a quantum system, and it is widely recognized as one of the defining features of quantum mechanics. Specifically, entanglement enables the implementation of powerful quantum protocols that can outperform classical systems in terms of computational power and communication security. Therefore, a thorough understanding of entanglement and the tools required to measure it is essential for investigating the behavior of quantum systems and designing practical quantum technologies. In this section, we aim to provide a detailed explanation of the most important entanglement measurements for pure and mixed states in the context of the 1D Heisenberg spin chain, which is a fundamental model system for studying many-body quantum mechanics.

2.3.1 Measure of Entanglement

This section provides an overview of entanglement measures for pure and mixed states. There are several measurements for entanglement based on whether the system is in a pure or mixed state. We first describe bipartite and multipartite pure states and introduce entanglement measures for them. After quantifying the entanglement in a pure state, we discuss how to calculate the level of entanglement in mixed states.

2.3.2 Coefficient Measurement for Pure States

The most well-known method to quantify entanglement for pure states is the entropy of entanglement. In addition to the entanglement entropy, we will discuss another measurement, the coefficient measure, for pure states, which is simpler than the entropy method, but the result is similar. In Chapter One, we found the quantity $|C_{++}C_{--} - C_{-+}C_{+-}|$ as an entanglement metric for a pure state. If this value is zero, the state is separable. If this value is non-zero, the state is entangled, and when it equals $\frac{1}{2}$, the state is maximally entangled. We can generalize this to a system with more than two parts. For example, consider a state with 5 parts:

$$|\psi\rangle = \frac{|+-\rangle - i|-+\rangle}{\sqrt{2}} \otimes \frac{|++-\rangle - i|+++\rangle - 2|--\rangle}{\sqrt{6}}.$$

The coefficients of this state are:

$$C_{+-++-} = \frac{1}{\sqrt{12}},$$

$$C_{+-+++} = \frac{-i}{\sqrt{12}},$$

$$C_{+----} = \frac{-2}{\sqrt{12}},$$

$$C_{-+++-} = \frac{-i}{\sqrt{12}},$$

$$C_{-++++} = \frac{-1}{\sqrt{12}},$$

$$C_{-+---} = \frac{2i}{\sqrt{12}}.$$

For the entanglement between particles 1 and 2, the coefficients $|C_{\alpha\beta}|^2 = \sum_{cde} |C_{\alpha\beta cde}|^2$, which gives:

$$C_{++} = 0\,,\; C_{+-} = \frac{1}{\sqrt{2}}\,,\; C_{-+} = \frac{1}{\sqrt{2}}\,,\; C_{--} = 0$$

$$C_{++}C_{--} - C_{-+}C_{+-} = \frac{1}{2}.$$

This means that particles 1 and 2 are maximally entangled. Now, we find the entanglement for particles 4 and 5.

$$C_{++} = \frac{1}{\sqrt{6}}\,,\; C_{+-} = \frac{1}{\sqrt{6}}\,,\; C_{-+} = 0\,,\; C_{--} = \frac{\sqrt{2}}{\sqrt{3}}$$

$$C_{++}C_{--} - C_{-+}C_{+-} = \frac{1}{3}.$$

This shows that particles 4 and 5 are entangled but less than particles 1 and 2. Now, we find the entanglement for particles 3 and 4.

$$C_{++} = \frac{1}{\sqrt{3}}\,,\; C_{+-} = 0\,,\; C_{-+} = 0\,,\; C_{--} = \frac{\sqrt{2}}{\sqrt{3}}$$

$$C_{++}C_{--} - C_{-+}C_{+-} = \frac{\sqrt{2}}{3}.$$

These two particles are entangled. Now, we study a case where two particles are not entangled, particles 1 and 5.

$$C_{++} = \frac{1}{\sqrt{12}}\,,\; C_{+-} = \frac{\sqrt{5}}{\sqrt{12}}\,,\; C_{-+} = \frac{1}{\sqrt{12}}\,,\; C_{--} = \frac{\sqrt{5}}{\sqrt{12}}$$

$$C_{++}C_{--} - C_{-+}C_{+-} = 0.$$

This demonstrates that particles 1 and 5 are not entangled and are separable.

2.3.3 Entropy of Entanglement

The entanglement entropy or entropy of entanglement is a measurement to find the degree of entanglement between two subsystems of a quantum system [33][34]. For a pure bipartite state, first, we need to find the density matrix for the bipartite pure state and then calculate the reduced density matrix for each subsystem to calculate the entanglement entropy as below:

$$S(\rho_A) = -Tr[\rho_A \log \rho_A] = -Tr[\rho_B \log \rho_B] = S(\rho_B). \tag{2.12}$$

Where $S(\rho_A)$ is the bipartite entanglement entropy for subsystem A, and $S(\rho_B)$ is the bipartite entanglement entropy for subsystem B. ρ_A and ρ_A are the reduced density

matrix for each part of the system.

2.3.4 Peres–Horodecki criterion

The Peres-Horodecki criterion, also known as the PPT criterion, serves as a necessary condition to determine whether a density matrix for a two-quantum system is separable or entangled. It functions as a witness of entanglement, meaning that it can identify whether a state is entangled or separable. It is important to note that while the PPT criterion is a witness of entanglement, it is not a measure of entanglement, as it only determines whether a state is entangled or separable, rather than quantifying the degree of entanglement [35].

Suppose we have a bipartite quantum state that acts on the Hilbert space $\mathcal{H}_A \otimes \mathcal{H}_B$ where $\mathcal{H}_A$ and $\mathcal{H}_B$ are two-dimensional. We represent this state by the density matrix ρ which can be written as:

$$\rho = \sum_{i,j,k,l} p_{kl}^{ij} |i\rangle\langle j| \otimes |k\rangle\langle l|, \tag{2.13}$$

where p_{kl}^{ij} are complex coefficients, and $|i\rangle$ and $|k\rangle$ are orthonormal bases for $\mathcal{H}_A$ and $\mathcal{H}_B$ respectively. Note that ρ is a 4×4 matrix in the tensor product space $\mathcal{H}_A \otimes \mathcal{H}_B$. Now, let's take the partial transpose of ρ with respect to the subsystem $\mathcal{H}_B$. This is denoted by ρ^{T_B} and can be obtained by transposing the second subsystem while leaving the first subsystem untouched. Mathematically, we can express this as:

$$\rho^{T_B} = (I_A \otimes T_B)(\rho),$$

where I_A is the identity operator acting on $\mathcal{H}_A$, and T_B is the transpose operator acting on $\mathcal{H}_B$. Explicitly, we have:

$$\rho^{T_B} = \sum_{i,j,k,l} p_{kl}^{ij} |i\rangle\langle j| \otimes |l\rangle\langle k|. \tag{2.14}$$

Note that ρ^{T_B} is also a 4×4 matrix, but its entries are obtained by transposing the second subsystem in ρ. The Peres-Horodecki criterion tells us that if ρ is separable (i.e., can be written as a convex combination of product states), then all the eigenvalues of ρ^{T_B} are non-negative. In other words, if there exists a negative eigenvalue

of ρ^{T_B}, then ρ must be entangled.

In summary, the Peres-Horodecki criterion provides a necessary condition for entanglement based on the partial transpose of the bipartite density matrix. If the partial transpose has a negative eigenvalue, then the state is entangled.

2.3.5 Mixed States

This section aims to present various measurements used to quantify entanglement for mixed states [36]. Entropy and coefficient measurements are not adequate for measuring entanglement in mixed states since they are designed for pure states. Instead, we explore measurements such as concurrence, entanglement of formation, and logarithmic negativity. We begin by describing what concurrence is and how to calculate concurrence. We then delve into the entanglement of formation and how to find it. Lastly, we examine logarithmic negativity, another measure of entanglement for mixed states [35].

2.3.6 Concurrence

Concurrence is a measure of entanglement between two qubits in a quantum system, particularly in the context of spin systems like the Heisenberg spin chain [37][38]. It was first introduced by Wootters in 1998 as a measure of entanglement [39]. A qubit is a quantum system with two levels, and can be used to represent a spin-1/2 particle, the polarization of a photon, or any other two-level quantum system. The concurrence takes values between 0 for a separable (non-entangled) state and 1 for a maximally entangled state, with higher values indicating greater entanglement between the two qubits. It provides a quantitative measure of the degree of entanglement between the two quantum systems with two levels and can be used to compare the entanglement of different states. The formula to calculate the concurrence is as below,

$$C(\rho) \equiv \max(0, \lambda_1 - \lambda_2 - \lambda_3 - \lambda_4), \tag{2.15}$$

where $\lambda_1, \lambda_2, \lambda_3, \lambda_4$ are the eigenvalues of R matrix, which is defined based on the density matrix, in decreasing order [40].

$$R = \sqrt{\sqrt{\rho}\tilde{\rho}\sqrt{\rho}}. \tag{2.16}$$

In the equation for the R matrix, we need to define $\tilde{\rho}$, which is the spin-flipped state of ρ,

$$\tilde{\rho} = (\sigma_y \otimes \sigma_y)\rho^*(\sigma_y \otimes \sigma_y), \tag{2.17}$$

where σ_y is one of the three Pauli spin matrices, and ρ^* is the complex conjugate of the density matrix. For multipartite mixed states, we need to take a partial trace and find the reduced density matrix to find the concurrence for each subsystem.

For instance, we calculated the density matrix for three spins in the Heisenberg chain in section 2.2. Now, in the present section, we can find the concurrence for each pair of spins:

$$\rho_{12} = \rho_{23} = \begin{pmatrix} 0.088 & 0 & 0 & 0 \\ 0 & 0.41 & -0.33 & 0 \\ 0 & -0.33 & 0.41 & 0 \\ 0 & 0 & 0 & 0.088 \end{pmatrix},$$

$$\rho_{13} = \begin{pmatrix} 0.33 & 0 & 0 & 0 \\ 0 & 0.17 & 0.16 & 0 \\ 0 & 0.16 & 0.17 & 0 \\ 0 & 0 & 0 & 0.33 \end{pmatrix},$$

where $\rho_{12}, \rho_{23}, \rho_{13}$ are the reduced density matrices between each pair of spins. The reduced density matrix for the nearest neighbors on the edge is the same,

$$R_{12} = R_{23} = \begin{pmatrix} 0.088 & 0 & 0 & 0 \\ 0 & 0.41 & -0.33 & 0 \\ 0 & -0.33 & 0.41 & 0 \\ 0 & 0 & 0 & 0.088 \end{pmatrix},$$

$$R_{13} = \begin{pmatrix} 0.33 & 0 & 0 & 0 \\ 0 & 0.17 & 0.16 & 0 \\ 0 & 0.16 & 0.17 & 0 \\ 0 & 0 & 0 & 0.33 \end{pmatrix}.$$

In this example, the reduced density and R matrix for each pair of spins are the same. The eigenvalues for each matrix are as below:

$$\lambda_i = [0.088, 0.088, 0.088, 0.74],$$

$$\lambda_j = [0.018, 0.33, 0.33, 0.33].$$

Where λ_i belongs to the nearest neighbors and λ_j belongs to the next nearest neighbors. Now, We can easily find the concurrence for each pair of spins:

$$C_{12} = C_{23} = 0.48, C_{13} = 0.$$

We can conclude that the nearest neighbors are entangled, and the next nearest neighbors are not entangled in this case without a magnetic field, fixed values of J = 1, and fixed $k_B T = 1$.

2.3.7 Entanglement of Formation

Entanglement of formation is another measure used to quantify entanglement in a quantum system, and it is based on concurrence. The formula for calculating the entanglement of formation is straightforward once the concurrence has been determined. Both of these measures are valuable tools for assessing the degree of entanglement present in a quantum system [37]. The entanglement of formation can be expressed using the following formula:

$$E_f = -(\frac{1+\sqrt{1-C^2}}{2}) \log_2 (\frac{1+\sqrt{1-C^2}}{2}) - (\frac{1-\sqrt{1-C^2}}{2}) \log_2 (\frac{1-\sqrt{1-C^2}}{2}). \tag{2.18}$$

This equation allows for the entanglement of formation to be easily calculated once the concurrence has been determined for a given pair of spins.

As an example, the reduced density matrices obtained in the previous section can

be used to determine the entanglement of formation for each pair of spins:

$$E_{f_{12}} = -(\frac{1+\sqrt{1-0.23}}{2})\log_2(\frac{1+\sqrt{1-0.23}}{2}) - (\frac{1-\sqrt{1-0.23}}{2})\log_2(\frac{1-\sqrt{1-0.23}}{2}) = 0.324,$$

$$E_{f_{23}} = -(\frac{1+\sqrt{1-0.23}}{2})\log_2(\frac{1+\sqrt{1-0.23}}{2}) - (\frac{1-\sqrt{1-0.23}}{2})\log_2(\frac{1-\sqrt{1-0.23}}{2}) = 0.324,$$

$$E_{f_{13}} = -(\frac{1+\sqrt{1-0}}{2})\log_2(\frac{1+\sqrt{1-0}}{2}) - (\frac{1-\sqrt{1-0}}{2})\log_2(\frac{1-\sqrt{1-0}}{2}) = 0.$$

While entanglement of formation and concurrence are different measures of entanglement, they are related such that the entanglement of formation can be expressed as a function of the concurrence for two-qubit states.

2.3.8 Negativity

Another measure to quantify entanglement that is introduced in this chapter is the logarithmic negativity [41]. The negativity of subsystem A can be defined in terms of the density matrix as below:

$$N(\rho) \equiv \frac{||\rho_A^T||_1 - 1}{2}. \tag{2.19}$$

Where ρ_A^T is the partial transpose of ρ for subsystem A. The trace norm operator of ρ , $||\rho||_1$ is defined as:

$$||X||_1 = \mathrm{Tr}|\mathrm{X}| = \mathrm{Tr}\sqrt{\mathrm{X}^\dagger\mathrm{X}}. \tag{2.20}$$

While the formula mentioned above is used to calculate the negativity of a subsystem, negativity is not necessarily a measure of entanglement. To obtain a quantitative measure of entanglement, we can instead compute the logarithmic negativity. The logarithmic negativity is closely related to negativity and can be derived from it.

Specifically, the logarithmic negativity can be obtained by taking the logarithm of the negativity of a given subsystem.

$$E_N(\rho) \equiv \log_2 ||\rho_A^T||_1 = E_N(\rho) \equiv \log_2 (2N + 1). \tag{2.21}$$

The logarithmic negativity can still be zero for certain entangled states, such as those that satisfy the positive partial transpose (PPT) criterion. Furthermore, unlike most other entanglement measures, the logarithmic negativity does not reduce to the entropy of entanglement on pure states. It is also important to note that the logarithmic negativity can take on values greater than one for maximally entangled states [41]. In Section 3.2, we compare the entanglement detection power of logarithmic negativity and concurrence. Both measures yield similar qualitative results, meaning they can detect the presence or absence of entanglement. However, they differ quantitatively in terms of their sensitivity to different types of entanglement.

2.4 Computational Tools

The computational analysis in this thesis relied on various tools to compute important quantities, such as the Hamiltonian and density matrices, as well as measures of entanglement. This section provides a description of the computational tools that were utilized to conduct the research presented in this thesis. By outlining the specific software packages used, this section aims to provide a comprehensive overview of the methods and techniques employed in this study.

2.4.1 Python

Python was the primary programming language used in this work. Python is a programming language widely used in scientific computing, data analysis, and machine learning. One of the main advantages of using Python in this work is the availability of several libraries specifically designed for mathematical computations, making it a useful tool for performing complex calculations and simulations. In the next section, we will provide a brief description of each Python library that was utilized in this study, highlighting their respective roles and functionalities in our analysis.

2.4.2 Python Libraries

Numpy [42], Matplotlib [43], and QuTiP [44][45] are the three python libraries that were used in this thesis to carry out the required computational tasks. Numpy was primarily used to perform various mathematical calculations, including the construction and manipulation of multi-dimensional arrays and matrices. For data visualization and plotting, Matplotlib was employed to generate 2D, scatter, and other types of plots. Additionally, QuTiP, an open-source computational library in python, specifically designed for quantum information physics, was utilized to model the quantum entanglement measurements. QuTiP has several advantages, including its compatibility with other widely used python libraries such as Numpy and Matplotlib, and its use of C and C++ extensions, which help reduce the computational time and cost. Further details and codes related to the implementation of these libraries are available in Appendix B.

Chapter 3

Model and Method

3.1 1D Heisenberg Model

The model that we use in this work is the one-dimensional Heisenberg spin chain. Werner Karl Heisenberg, a German theoretical physicist, introduced the quantum Heisenberg model, which is a statistical mechanical model for studying critical points and phase transitions of magnetic systems in which the spins of the magnetic systems are treated quantum mechanically. We can write the Hamiltonian of the one-dimensional Heisenberg spin chain as,

$$H = \sum_{i=1}^{N-1} J_x S_x^i S_x^{i+1} + J_y S_y^i S_y^{i+1} + J_z S_z^i S_z^{i+1} - \sum_{i=1}^{N} B S_z^i, \tag{3.1}$$

where B is the external magnetic field, J_x, J_y, and J_z are coupling constants, and S_x, S_y, and S_z are spin 1/2 operators for the ith spin. There are several types of the Heisenberg model depending on the values of J_x, J_y, and J_z. The first case is where $J_x = J_y = J_z$; the model is called the XXX-model [21][29]. As all coupling constants are equal, in this case, the physics of the system only depends on the sign of the J. The second case is the XXZ-model [29]. In this case, $J = J_x = J_y \neq J_z$. In the final case, if all components of the coupling constants are different, $J_x \neq J_y \neq J_z$, the model is called the XYZ-model [29].

3.2 Entanglement measure selection

In this section, we compare the concurrence and logarithmic negativity for quantifying entanglement for a chain of spins on the one-dimensional XXX Heisenberg model. Both the concurrence and logarithmic negativity measures of entanglement provide similar results and are useful measures for quantifying entanglement in the 1D Heisenberg spin chain. While the general trends in entanglement are qualitatively similar for different pairs of spins, there are quantitative differences in the values obtained for the concurrence and logarithmic negativity measures. In Fig. 3.1, both measures show that the nearest neighbor spins on the edges are entangled without a magnetic field, and entanglement is present between all spin pairs in the critical magnetic field range in which significant changes in entanglement occur. Similarly, in the high-temperature case shown in Fig. 3.2, both measures show that the general trends for the presence of entanglement are the same, but there are differences in the entanglement values obtained for certain spin pairs. It is important to mention that the differences in the entanglement values are expected due to the different mathematical properties of the measures. Our findings indicate that the concurrence measure exhibits higher values compared to the logarithmic negativity.

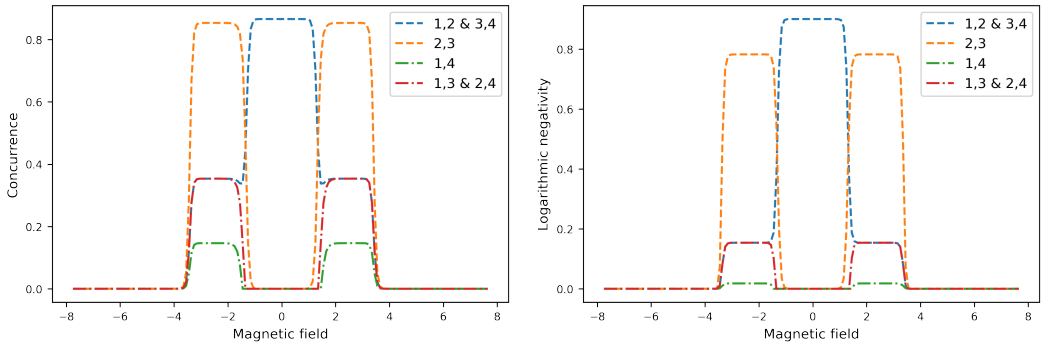

(a) (b)

Figure 3.1: Low temperature nearest neighbors entanglement in the XXX Heisenberg model with 4 spins measured by (a) concurrence, (b) logarithmic negativity, for $k_BT = 0.1$, $J = 1$, $N = 4$.

In this work, our focus is on quantifying entanglement in the 1D Heisenberg spin chain, specifically for two spins in the chain with varying chain lengths. To achieve this, we will be using the concurrence measure of entanglement. The concurrence is

well-suited for bipartite systems such as our case, where we are interested in quantifying the entanglement between two spins in the chain. Several previous studies have also used the concurrence measure to quantify entanglement in spin systems, including the 1D Heisenberg spin chain [46][47][48][49]. Therefore, we believe that using the concurrence measure will provide us with more useful results than the other measure.

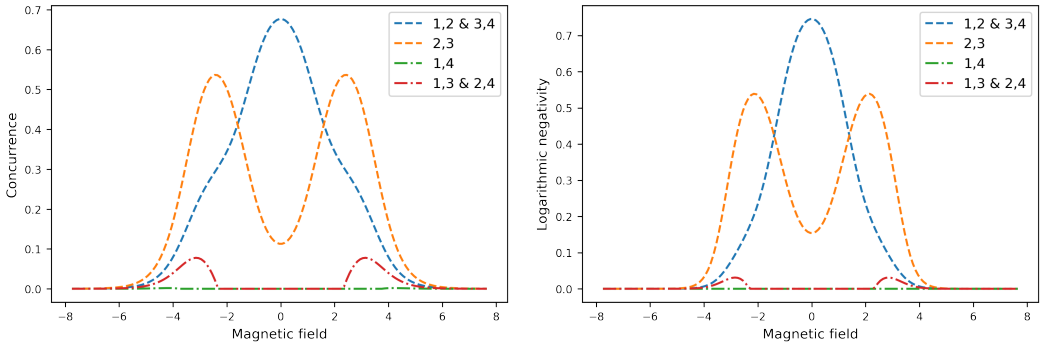

(a) (b)

Figure 3.2: High temperature nearest neighbors entanglement in the XXX Heisenberg model with 4 spins measured by (a) concurrence, (b) logarithmic negativity, for $k_BT = 1$, $J = 1$, $N = 4$.

Chapter 4

Results and Discussion

4.1 Entanglement without magnetic field

4.1.1 Entanglement as a function of coupling constants

In this section, we investigate the entanglement of the Heisenberg model without any external magnetic field, equation (2.3) for $B = 0$, for different numbers of spins between the nearest neighbors located at the edge of the chain. Firstly, we fix the temperature and change the coupling constants to find the impact of the coupling on the entanglement in the absence of the magnetic field.

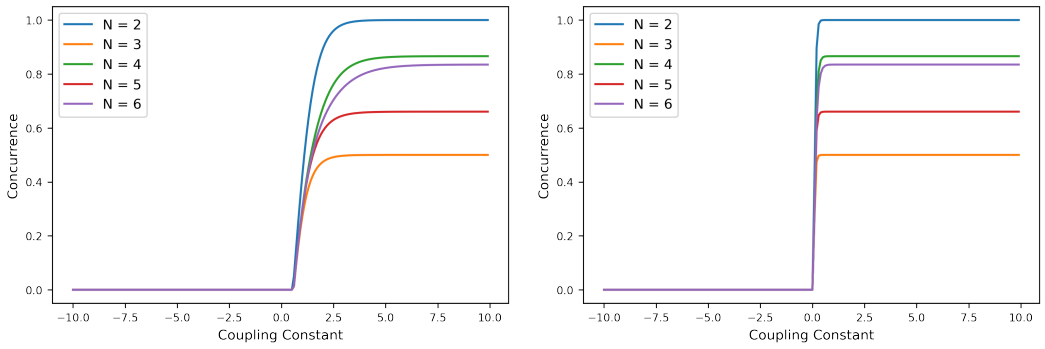

(a) (b)

Figure 4.1: Concurrence vs. coupling constants for $B = 0$, $J = [-10, 10]$, nearest neighbors spins (1,2), (a): $k_B T = 2$, (b): $k_B T = 0.1$.

In Fig. 4.1, all coupling constants are equal and varied from $J = -10$ to $J = 10$

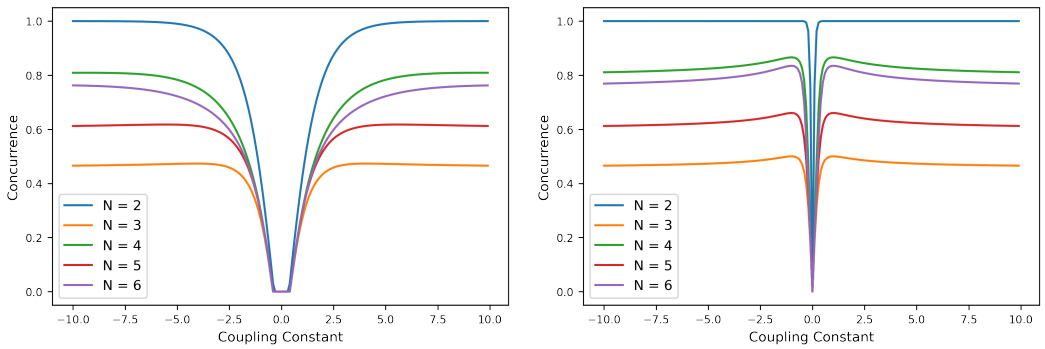

(a) (b)

Figure 4.2: Concurrence vs. coupling constants for $B = 0$, $J_x = J_y = [-10, 10]$, $J_z = 1$, nearest neighbors spins (1,2), (a): $k_BT = 2$, (b): $k_BT = 0.1$.

without an external magnetic field. The concurrence is zero for the ferromagnetic case, $J < 0$, and it starts to increase for the antiferromagnetic case, $J > 0$. Fig. 4.1(a) shows the high-temperature result, $k_BT = 2$, while Fig. 4.1(b) is for lower temperature case, $k_BT = 0.1$. In both cases, the concurrence converges to a maximum value that depends on the number of spins in the chain. The convergence is faster at lower temperatures.

In Fig. 4.2, the value of J_z is set to 1, and J_x and J_y vary between -10 to 10. Fig. 4.2(a) represents the high-temperature limit, $k_BT = 2$, but Fig. 4.2 (b) is for low temperature, $k_BT = 0.1$. The concurrence is zero for $J = 0$, and it rapidly increases for $|J| > 0$. The graphs are symmetric about $J = 0$. For $|J| > 0$, the concurrence converges to different values depending on the number of spins in the chain, N, with faster convergence at low temperatures. The curves show a small peak for $J \approx 1$ at low temperatures for more than two spins in the chain.

In Fig. 4.3, $J_z = 1$, $J_x = 0$, and J_y varies from -10 to 10. Fig. 4.3(a) represents the high-temperature limit of $k_BT = 2$, while Fig. 4.3(b) shows the lower temperature limit of $k_BT = 0.1$. Fig. 4.3 illustrates the dependence of concurrence on the coupling strength J_y, where it is zero at zero coupling and increases with increasing J_y. When the system is composed of more than two spins, a maximum concurrence is observed at around $J_y \approx 3$ for the high-temperature limit, as shown in Fig. 4.3(a). However, as the temperature decreases, the maximum value of concurrence shifts to smaller values of J_y, approximately $J_y \approx 2$. Interestingly, for large values of J_y, the concurrence approaches very small values.

Figs. 4.1, 4.2, and 4.3 demonstrate that the concurrence is dependent on the number of spins in the chain. The graphs reveal that the largest concurrence occurs when $N = 2$, while the smallest is observed when $N = 3$. Interestingly, the behavior of the concurrence with respect to N differs for odd and even values. Specifically, the concurrence decreases with increasing N when N is even, but increases when N is odd.

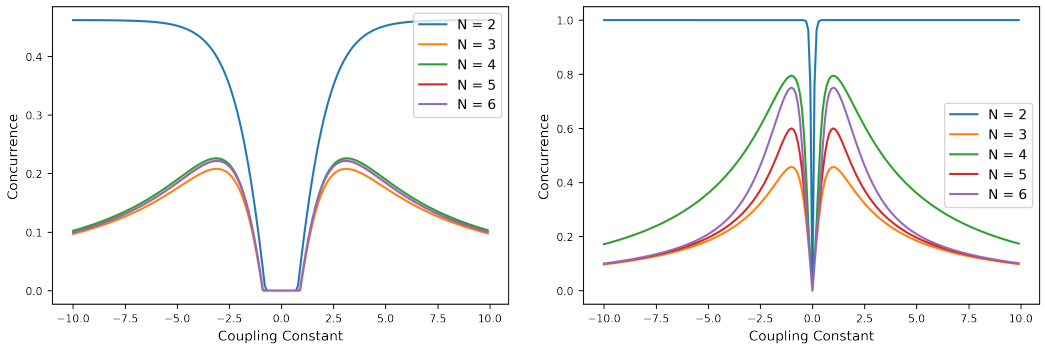

(a) (b)

Figure 4.3: Concurrence vs. coupling constants for $B = 0$, $J_x = 0$, $J_y = [-10, 10]$, $J_z = 1$, nearest neighbors spins (1,2), (a): $k_B T = 2$, (b): $k_B T = 0.1$.

4.1.2 Entanglement as a function of temperature

In the present section, we examine the relationship between temperature and concurrence.

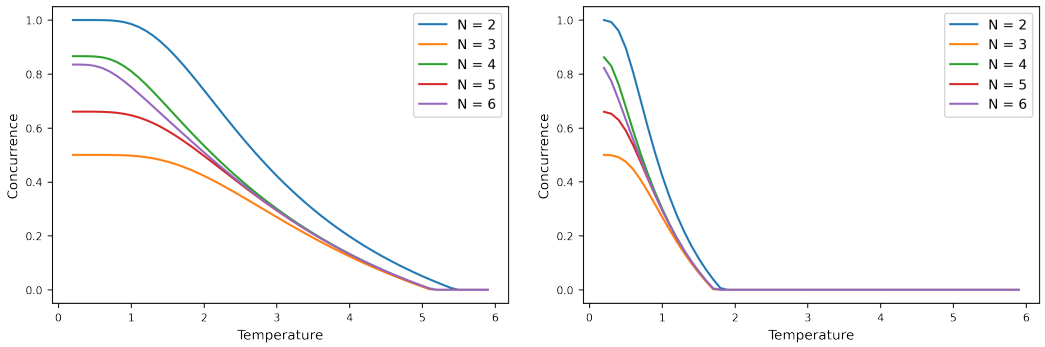

(a) (b)

Figure 4.4: Concurrence vs. temperature for $B = 0$, nearest neighbors, spins (1,2), (a)$J = 1.5$, (b) $J = 0.5$.

In Fig. 4.4(a), we depict the behavior of concurrence as a function of temperature for fixed values of the coupling constants $J_x = J_y = J_z = 1.5$, without an external magnetic field ($B = 0$). The results show that the concurrence exhibits a maximum at very low temperatures and decreases to zero as the temperature increases. Moreover, the concurrence vanishes between $k_BT = 5$ and $k_BT = 6$ for all system sizes, as illustrated in Fig. 4.4(a). Conversely, when the coupling constants are weakened to $J_x = J_y = J_z = 0.5$, the concurrence decreases more rapidly, as seen in Fig. 4.4(b), and disappears at around $k_BT = 1.8$. Generally, in the antiferromagnetic case with all positive coupling constants, the concurrence increases with increasing coupling constants, while it decreases with increasing temperature.

4.1.3 Entanglement without magnetic field: Discussion

The fact that the concurrence for the Heisenberg ferromagnetic case is zero at all temperatures can be explained by the absence of entanglement in ferromagnetic systems. This is because, in the ferromagnetic case without an external magnetic field, the ground state of the 1D Heisenberg spin chain is a product state in which all spins are aligned in the same direction. This means that the spins are not entangled with each other.

The peak in concurrence with respect to coupling strength and subsequent decrease in the cases in which coupling constants are a combination of positive and negative values can be explained by the competition between the strength of coupling and the thermal effects. At small coupling strengths, the thermal effects dominate, and entanglement is low. As the coupling strength increases, the entanglement increases due to the dominance of the interaction term. However, as the coupling strength becomes too strong, the competition between the strength of coupling and thermal effects is not the only factor influencing the behavior of entanglement in this system. Other factors, such as the specific values and combinations of coupling constants, can also play a significant role.

The decrease in concurrence with increasing temperature can be attributed to the fact that as the temperature increases, the system becomes more disordered and the thermal fluctuations increase. This makes it more difficult for the spins to be entangled, leading to a decrease in entanglement. This behavior is expected in many physical systems where entanglement is lost at high temperatures.

The increase in concurrence with increasing coupling constants in the antiferromagnetic case suggests that entanglement can be tuned by varying the coupling strength. This has potential applications in quantum information processing, where the control of entanglement is crucial. The convergence of concurrence to a different value depending on the number of spins suggests that the even and odd numbers of spins behave differently (because of the Kramers' theorem), which can be important in the design of quantum devices based on spin systems.

4.2 Entanglement in the presence of a magnetic field

This section aims to investigate the effect of an external magnetic field on the concurrence in the 1D Heisenberg spin chain. Additionally, we aim to examine the entanglement of different pairs of spins in the chain and check the results with the eigenvalues of the Hamiltonian and R-matrix.

In the subsequent section, we explore the concurrence in the 1D Heisenberg spin chain with varying numbers of spins, including two, three, four, and five spins. The concurrence is plotted against the magnetic field for three different temperature ranges: high ($k_BT = 2$), medium ($k_BT = 1$), and low ($k_BT = 0.1$). The coupling constants in all three temperature ranges are set to $J = 1$, which corresponds to the antiferromagnetic case.

4.2.1 Two spins

In this particular section, our focus is on analyzing the concurrence in the 1D Heisenberg spin chain consisting of only two spins. This simplified scenario enables us to study the entanglement exclusively between the nearest neighbors in the chain.

As shown in Fig. 4.5, the concurrence decreases with increasing magnetic field. The concurrence peaks when the magnetic field is zero. For $k_BT = 2$, Fig. 4.5(a), we see that the maximum of the concurrence is $C \approx 0.42$ and vanishes at $B \approx 7.5$. In Fig. 4.5(b), we plot the concurrence versus magnetic field for $k_BT = 1$. In this case, the maximum concurrence is almost 0.85, and the concurrence vanishes at around $B = 4$.

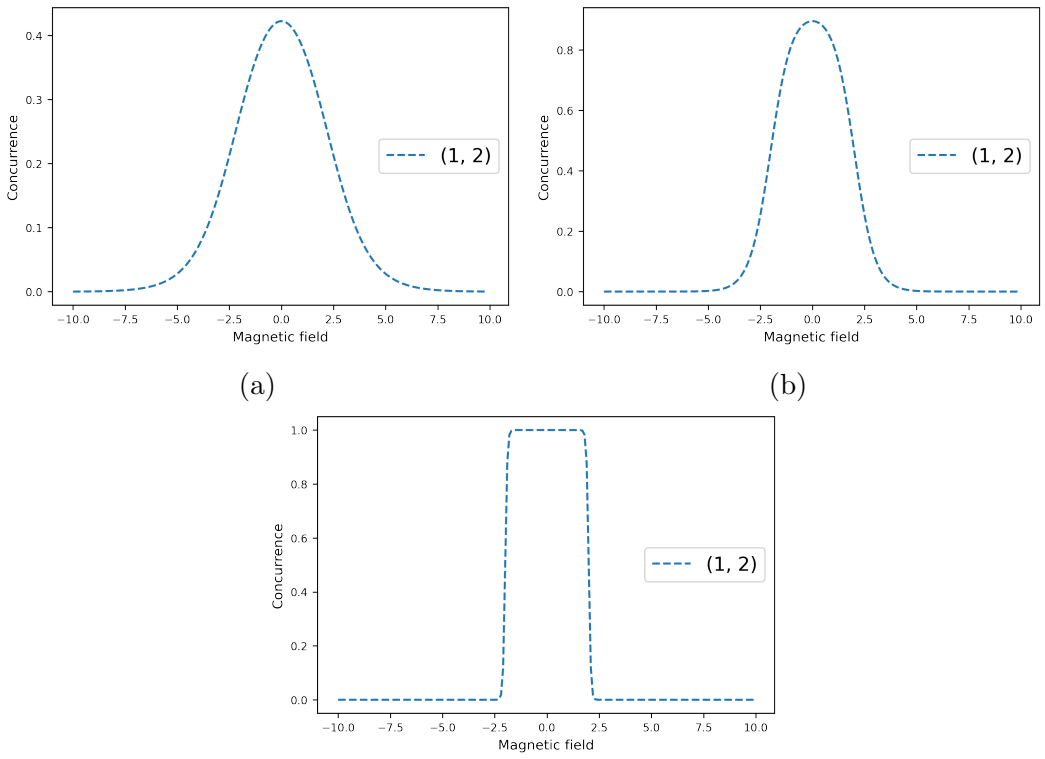

Figure 4.5: Concurrence vs. magnetic field for two spins, $J_x = J_y = J_z = 1$, (a): $k_BT = 2$; (b): $k_BT = 1$; (c): $k_BT = 0.1$.

In Fig. 4.5(c), we plot the concurrence versus magnetic field for the low-temperature, $k_BT = 0.1$. The concurrence is maximum from $B = 0$ to $B = 2.5$, then it significantly decreases and vanishes.

Generally, we can say that the maximum for the concurrence increases by decreasing temperature, but the width of the maximum decreases. Another result is that the concurrence vanishes more quickly for lower temperatures.

In Fig. 4.6, we plot the eigenvalues of the Hamiltonian of the Heisenberg spin chain with two spins versus magnetic field. For zero external magnetic field, there are a triplet and a singlet. After applying an external magnetic field, the degeneracy of the triplet is lifted, and the triplet and singlet states mix together.

In Figures 4.7(a) and 4.7(b), we depict the eigenvalues of the R-matrix utilized for calculating the concurrence at both high and low temperatures. We observe that, in both temperature regimes, the triplet state of the Hamiltonian corresponds to

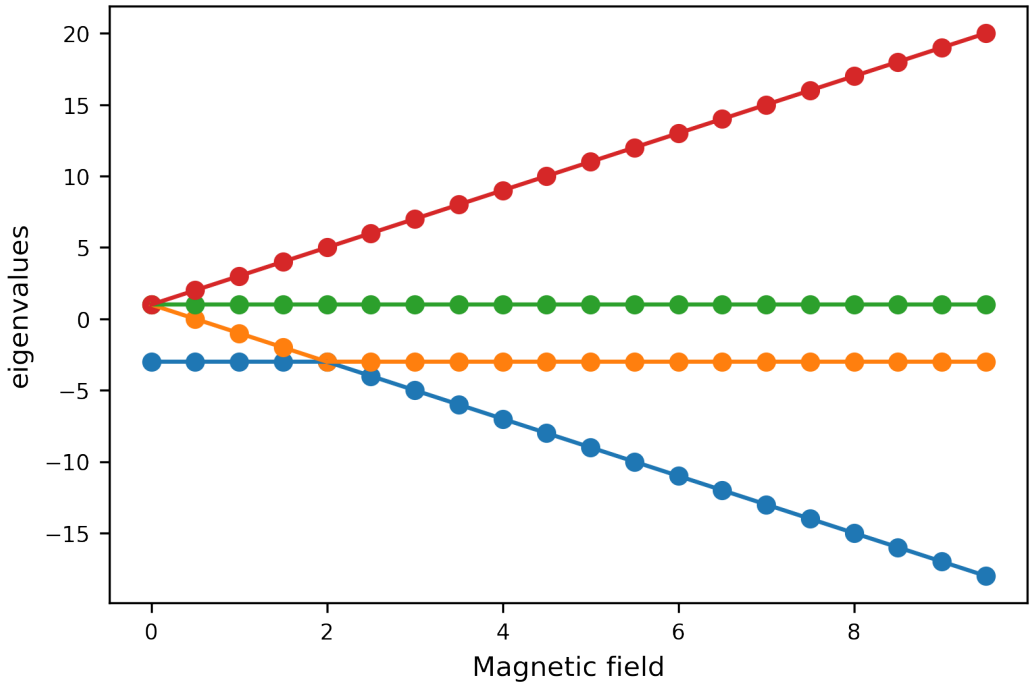

Figure 4.6: Eigenvalues of Hamiltonian vs. magnetic field for $N = 2$.

triply degenerate zero eigenvalues, while the singlet state is solely responsible for the entanglement. In Figure 4.7, an increase in the magnetic field leads to a decrease in the magnitude of the eigenvalue for the non-degenerate state, signifying a reduction in the concurrence within this range. The maximum slope of Figure 4.7 occurs at $B \approx 2$, where there is a level crossing in the eigenvalues of the Hamiltonian, as demonstrated in Figure 4.6. At high values of B, the spins align with the direction of B, resulting in the vanishing of the concurrence.

4.2.2 Three spins

This section of the thesis focuses on investigating the concurrence of the spin chain that comprises three spins. The inclusion of the third spin allows us to extend our analysis beyond the concurrence between the nearest neighbors on the edge of the chain, i.e., spins (1,2) and (2,3), to also examine the concurrence between the next-nearest neighbors, spins (1,3). Such an investigation holds critical significance in the context of my thesis.

In Figure 4.8, we observe that for a spin chain, the concurrence between nearest

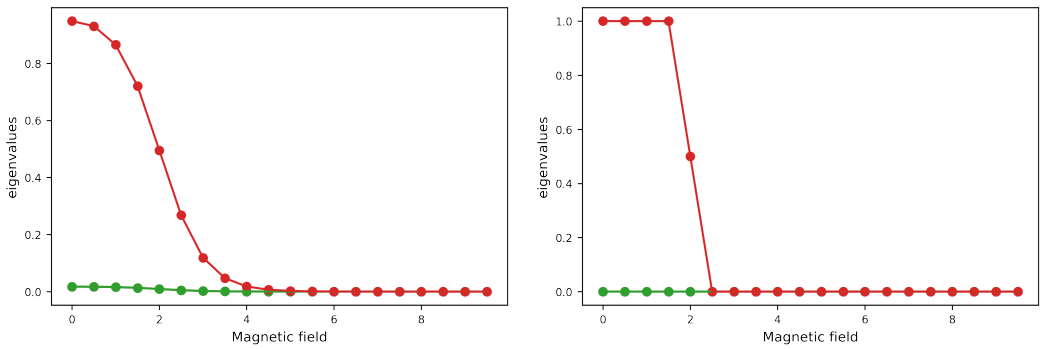

(a) (b)

Figure 4.7: Eigenvalues of the R-matrix vs. magnetic field for $N = 2$, (a): $k_BT = 1$; (b): $k_BT = 0.1$.

neighbor spins (1,2) and (2,3) is equal since both sets are located at the edge of the chain. However, the concurrence between the next-nearest neighbor spins (1,3) is lower than that of the nearest neighbors. At high temperature, where $k_BT = 2$, the concurrence between nearest neighbors on the edge decreases as the magnetic field increases, as depicted in Figure 4.8(a). A slight dip in concurrence is observed at $B = 0$. On the other hand, the concurrence between next-nearest neighbors is zero for all magnetic field values. At a lower temperature of $k_BT = 1$, as shown in Figure 4.8(b), the maximum concurrence between nearest neighbors increases from 0.28 to 0.55, and the concurrence vanishes at approximately $B = 5$, compared to $B = 7.5$ in the $k_BT = 2$ case. For the next-nearest neighbors, concurrence is zero when the magnetic field is zero, but there is a non-zero concurrence for the critical range of magnetic field values, $B = 2$ to $B = 5$, where the concurrence changes significantly, and it goes to zero for $B > 5$. In Figure 4.8(c), the concurrence is plotted for the low-temperature case, $k_BT = 0.1$. In this case, the maximum value for concurrence between nearest neighbors is 0.65, the highest value compared to the higher temperature cases, $k_BT = 2$ and $k_BT = 1$. The concurrence has a maximum value from $B = 0$ to $B = 3$ and then goes to zero. The trend of concurrence for next-nearest neighbor spins is similar to that of nearest neighbors, but with a lower level of concurrence.

Generally, for three spins in the chain, we can mention the maximum value of the concurrence increases as temperature decreases, but the range for the magnetic field that the system is entangled decreases. Like two spins system, the rate at which

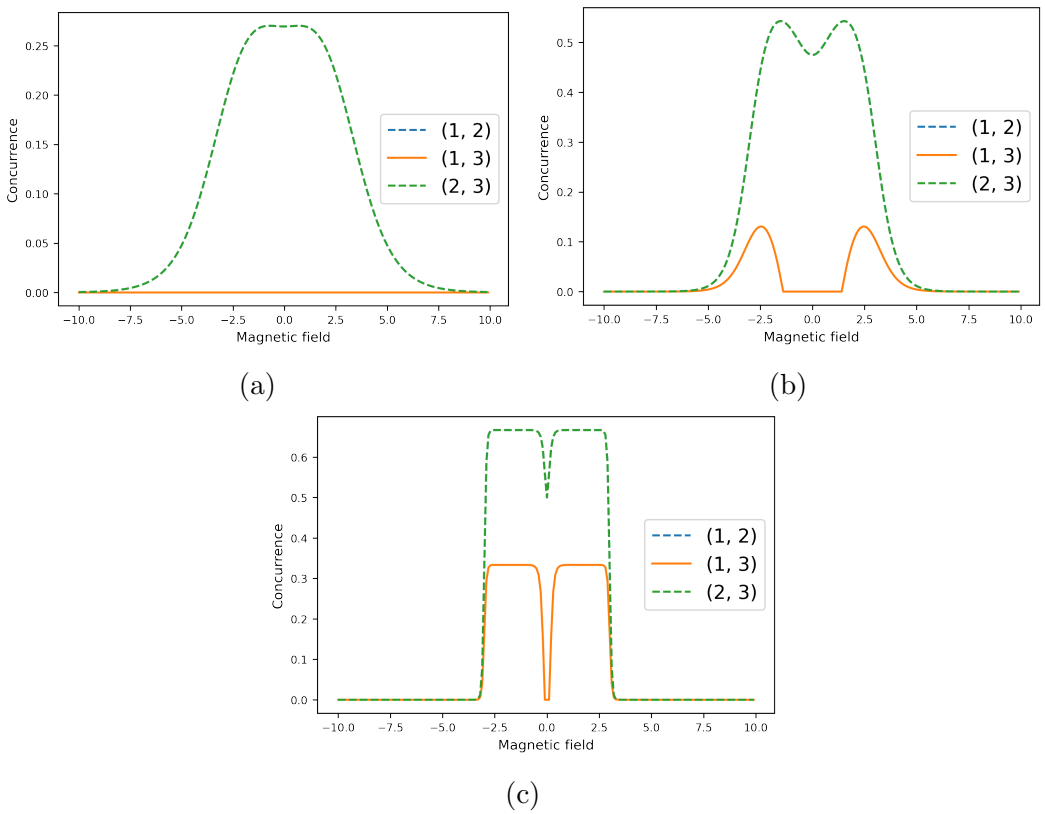

Figure 4.8: Concurrence vs. magnetic field for $N = 3$, $J_x = J_y = J_z = 1$, (a): $k_BT = 2$; (b): $k_BT = 1$; (c): $k_BT = 0.1$.

the concurrence vanishes for the lower temperature case is more than the higher temperature. Finally, the last result of this section is that the concurrence for the nearest neighbors is more than the next-nearest neighbors.

In Fig. 4.9, we plot the eigenvalues of the Hamiltonian of the Heisenberg spin chain with three spins as a function of magnetic field. When the external magnetic field is zero, there are two doublets and one quartet. Upon applying an external magnetic field, the degeneracy lifts, and there are some level crossings between the eigenvalues of the Hamiltonian from $B = 0$ to almost $B = 5$. This is the range of the magnetic field for which we find a non-zero concurrence.

Figure 4.10 examines the eigenvalues of the R-matrix for the nearest and next-nearest neighbors to check the concurrence outcome. At $B = 0$, two degenerate eigenvalues are present in both cases. Specifically, for the nearest neighbors, the concurrence is determined by a single, sizeable eigenvalue of the R-matrix. On the

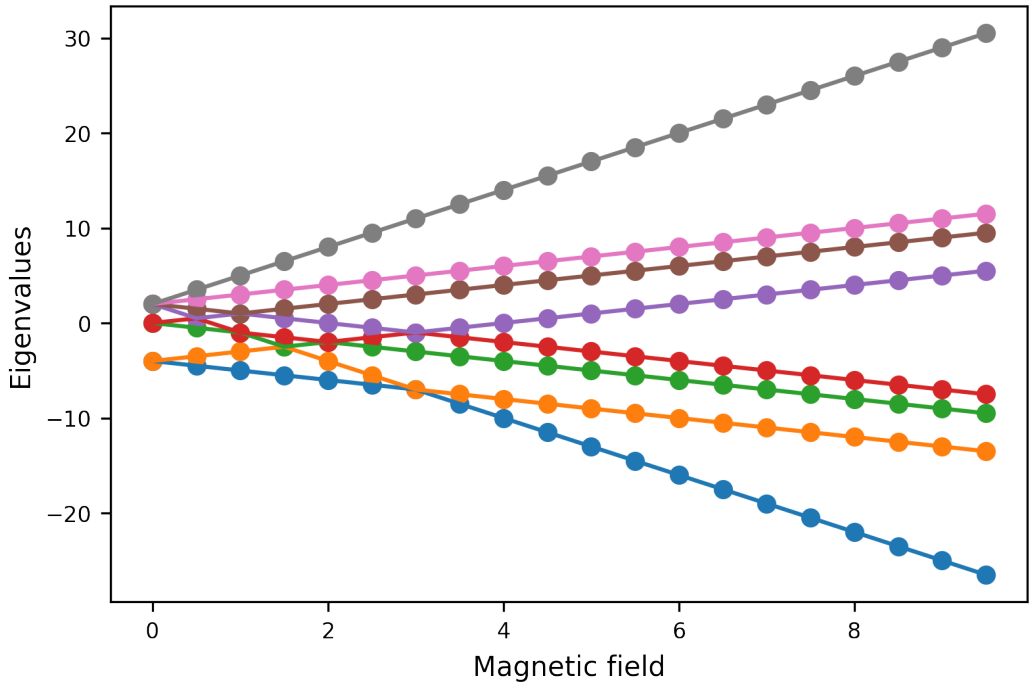

Figure 4.9: Eigenvalues of Hamiltonian vs. magnetic field for $N = 3$.

other hand, for next-nearest neighbors, the largest eigenvalue of the R-matrix is doubly degenerate at $B = 0$, resulting in the concurrence vanishing at this point.

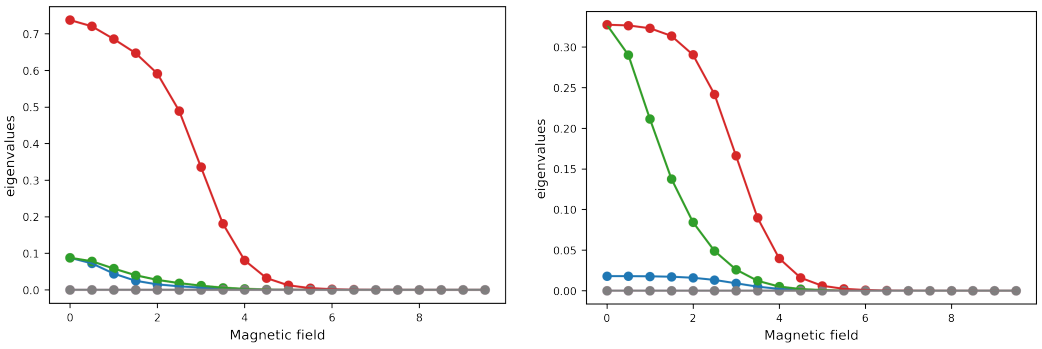

(a) (b)

Figure 4.10: Eigenvalues of the R-Matrix vs. magnetic field for $N = 3$, $k_B T = 1$, (a): spins (1,2); (b): spins(1,3).

4.2.3 Four Spins

This section of the thesis focuses on exploring the concurrence in the 1D Heisenberg spin chain that consists of four spins. This scenario bears similarity to the previous case with three spins, with the added complexity of considering the entanglement between the nearest neighbors in the middle of the chain, i.e., spins (2,3). Moreover, we examine the concurrence between the next-nearest neighbors, spins (1,3) and (2,4), and introduce a new scenario involving the next-next-nearest neighbors, i.e., spins (1,4), the spins in the first and last places of the chain.

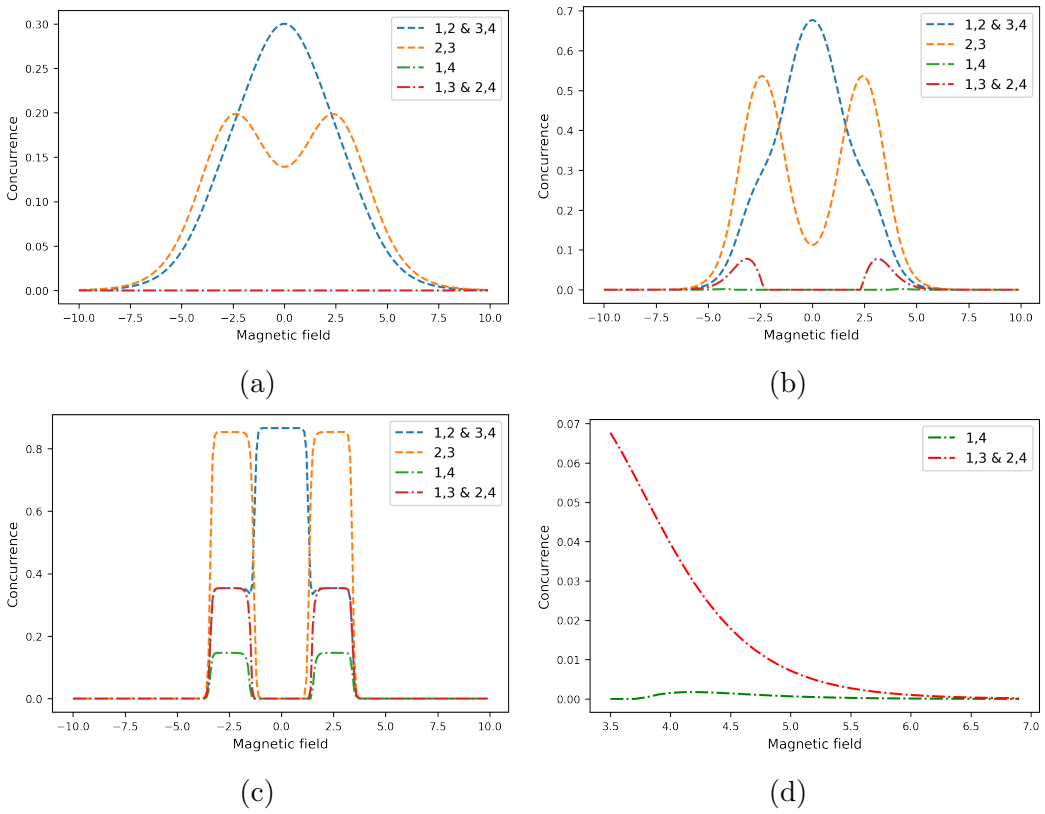

Figure 4.11: Concurrence vs. Magnetic field for $J_x = J_y = J_z = 1$, $N = 4$, (a): $k_BT = 2$; (b): $k_BT = 1$; (c): $k_BT = 0.1$; (d): zoom range for $k_BT = 1$

In Fig. 4.11, the concurrence between the nearest neighbor spins on the edges of the chain, spins (1,2) and (3,4), is identical due to the symmetry of the system. The maximum concurrence for the nearest neighbor spins in the middle of the chain, spins (2,3), is found to be less than those at the edges, while the concurrence between the next-nearest neighbor spins, spins (1,3) and (2,4), is identical due to symmetry but less

than the concurrence between the nearest neighbors. Additionally, the concurrence between the first and last spins in the chain, spins (1,4), is the lowest.

In Fig. 4.11(a), it is observed that the concurrence for the nearest neighbor spins at the edges has a maximum value at zero magnetic field, which decreases with increasing magnetic field and disappears at around $B = 8$. A dip in the concurrence is observed for spins (2,3), the nearest neighbors in the middle of the chain, at $B = 0$. The concurrence then decreases and approaches zero at a magnetic field value that is almost the same as that of the spins at the edges of the chain. The concurrence for the next-nearest and next-next-nearest neighbor spins at $k_BT = 2$ is zero for all magnetic field values.

By considering a lower temperature of $k_BT = 1$ in Fig. 4.11(b), it is observed that the maximum concurrence for the nearest neighbor spins increases, and the concurrence vanishes at around $B = 6$, compared to $B = 8$ for the higher-temperature case. A small level of concurrence is also observed for the next-nearest neighbor spins in the critical range of the magnetic field, $B = 2$ to $B = 5$. In Fig. 4.11(d), a low level of concurrence is observed within the critical range of the magnetic field for spins (1,4).

In the lowest temperature case of $k_BT = 0.1$ shown in Fig. 4.11(c), the maximum value of the concurrence for all pairs of spins is larger than the high-temperature cases. The concurrence dramatically changes within the magnetic field range from $B = 1.8$ to $B = 3.8$. Before and after this range, the concurrence rapidly decreases. The concurrence for the next-nearest neighbor spins is zero just below this range and suddenly goes to a maximum, which remains until the end of the range of the magnetic field, and then rapidly disappears at the end of this range. Notably, there is a noticeable level of concurrence for spins (1,4) within the range of the magnetic field in the low-temperature limit of $k_BT = 0.1$.

To summarize, in the case of four spins in the Heisenberg spin chain, we can conclude that the maximum value of the concurrence increases as the temperature decreases, but the range of the magnetic field in which the system is entangled decreases. Like the two and three-spin systems, the concurrence vanishes faster for the lower temperature case compared to the higher temperature values. Finally, the last result of this section is that the concurrence decreases as the number of lattice sites between given spins in the chain increases.

In Fig. 4.12, we plot the eigenvalues of the Hamiltonian with four spins versus

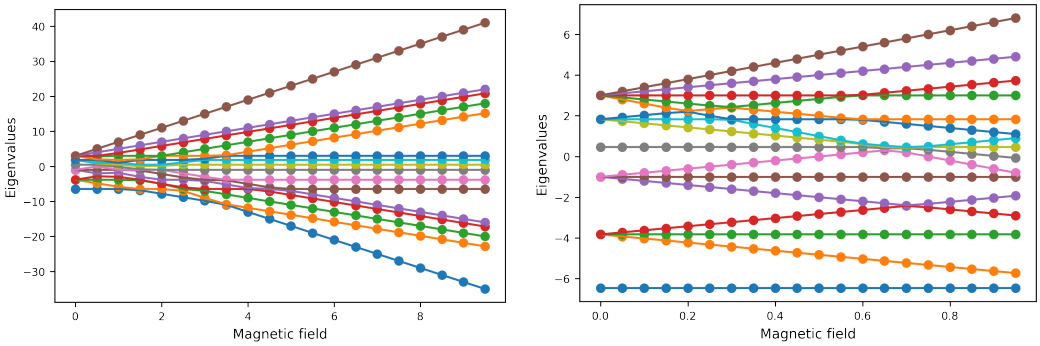

(a) (b)

Figure 4.12: Eigenvalues of Hamiltonian vs. magnetic field for $N = 4$.

magnetic field. In the absence of an external magnetic field, there is one five-fold degeneracy, three three-fold degeneracy, and two singlets. After applying an external magnetic field, the degeneracies lift. We can see some level crossings of eigenvalues from $B = 0$ to almost $B = 4$, which is the range of the magnetic field for which we find some fluctuations in the concurrence.

Figure 4.13 displays the eigenvalues of the R-matrix for four spins, considering nearest and next-nearest neighbors, respectively. For nearest neighbors, as illustrated in Figure 4.13(a), the non-degenerate largest eigenvalue at $B = 0$ and the triply degenerate smallest eigenvalue results in a considerable concurrence at low magnetic fields. In the case of next-nearest neighbors, depicted in Figure 4.13(b), the doubly-degenerate largest eigenvalue at $B = 0$ leads to a concurrence of zero at low magnetic field strengths. However, in the range of magnetic fields from $B \approx 1$ to $B \approx 4$, the disparity between these two large eigenvalues intensifies, resulting in a non-zero concurrence.

4.2.4 Five Spins

The objective of this particular section is to investigate the concurrence of the spin chain with five spins. This situation introduces a novel scenario, as we explore the entanglement between all spin pairs for four spins in the chain, in addition to examining the concurrence between the first and last spin of the chain, i.e., spins (1,5), which are separated by a large number of lattice sites.

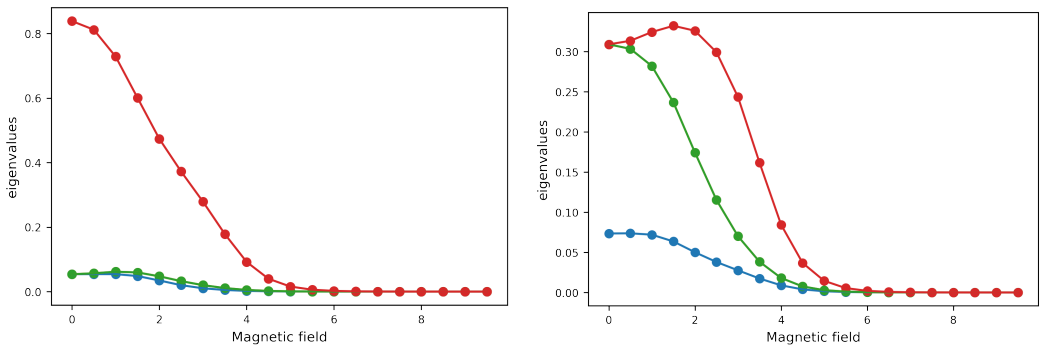

(a) (b)

Figure 4.13: Eigenvalues of R-Matrix vs. magnetic field for $N = 4$, (a): spins (1,2); (b): spins(1,3).

In Fig. 4.14(a), it is observed that at $k_BT = 2$, the concurrence between next-nearest neighbors is negligible. The concurrence is only noticeable for the nearest neighbors, both at the middle and edges of the chain. However, Fig. 4.14(b) illustrates that by reducing the temperature from $k_BT = 2$ to $k_BT = 1$, the concurrence for next-nearest neighbors, such as spins (1,3), spins (3,5), and spins (2,4), becomes non-zero. As expected, the level of concurrence decreases with an increase in the number of lattice sites between the given pairs. The concurrence remains negligible for the first and last spins on the chain and for the next-next-nearest neighbors, spins (1,4) and spins (2,5). In Fig. 4.14(c), the concurrence for five spins in the low-temperature regime, $k_BT = 0.1$, is depicted. There is a magnetic field range between $B = 2$ to $B = 4$ where some pairs of spins exhibit a maximum level of concurrence, except for the nearest neighbors at the edges. In this low-temperature case, even the first and last spins on the chain display entanglement within this range of the magnetic field.

In Fig. 4.15, we plot the eigenvalues of the Hamiltonian for five spins. Without an external magnetic field, there are one six-fold degeneracy, four four-fold degeneracies, and five double-degeneracies. After applying an external magnetic field, the degeneracies lift, and there are some level crossings of the eigenvalues from $B = 0$ to almost $B = 6$; this is the critical range of the magnetic field where concurrence changes significantly. In Figure 4.16(a), the largest eigenvalue of the R matrix for nearest neighbors is non-degenerate at $B = 0$, while the smallest eigenvalue is triply degenerate, resulting in a non-zero concurrence at low magnetic fields. Conversely, for next-nearest neighbors, as shown in Figure 4.16(b), the largest eigenvalue of the

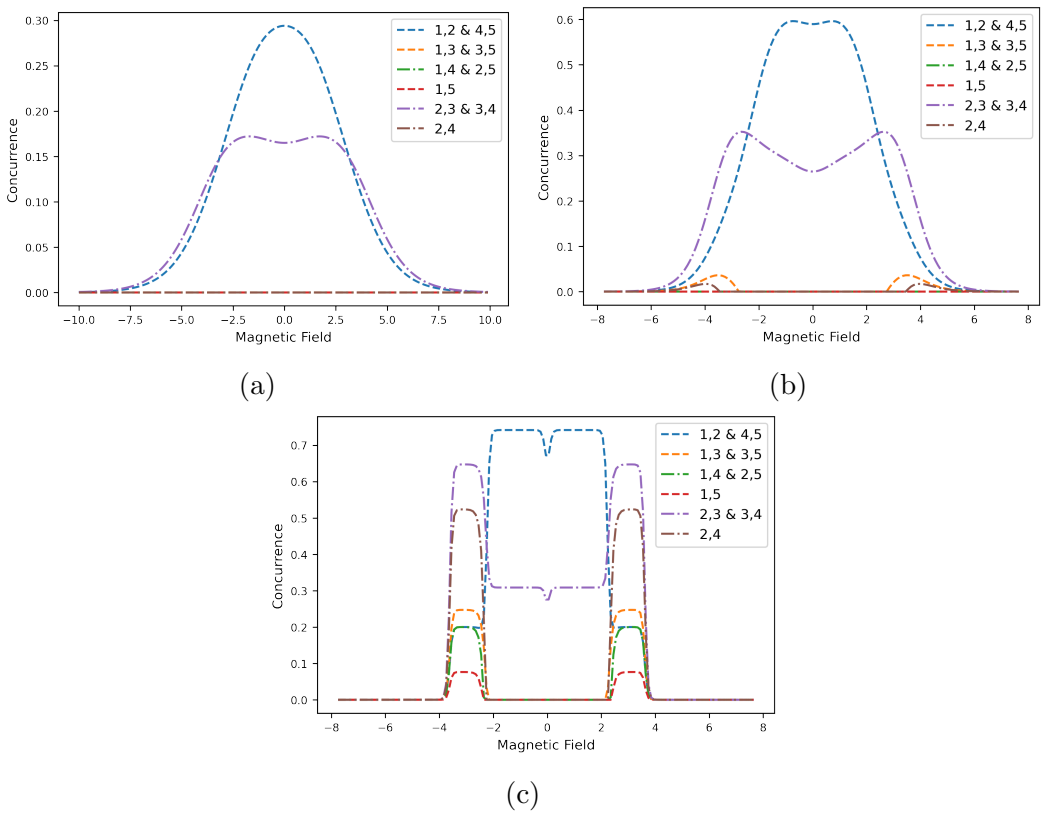

(a) (b)

(c)

Figure 4.14: Concurrence vs. magnetic field for $J_x = J_y = J_z = 1$, $N = 5$, (a): $k_BT = 2$; (b): $k_BT = 1$; (c): $k_BT = 0.1$.

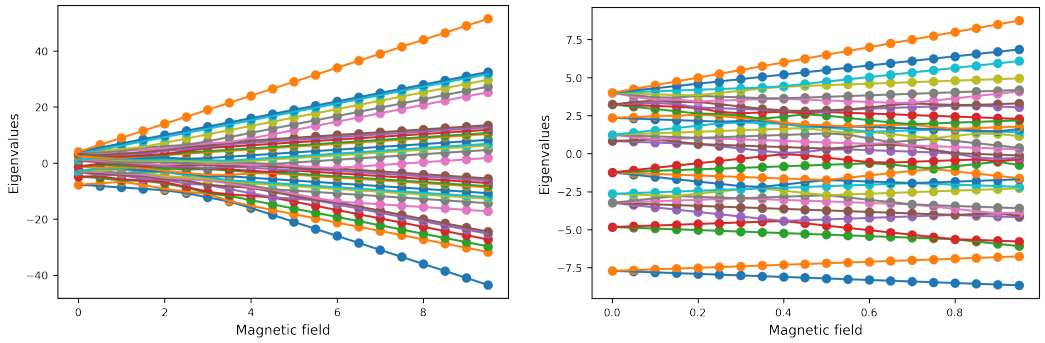

(a) (b)

Figure 4.15: Eigenvalues of Hamiltonian vs. magnetic field for $N = 5$.

R matrix is doubly degenerate at $B = 0$, leading to a vanishing concurrence at low magnetic field strengths. However, the disparity between these two large eigenvalues increases in the magnetic field range from $B \approx 2$ to $B \approx 4$, resulting in a non-zero concurrence.

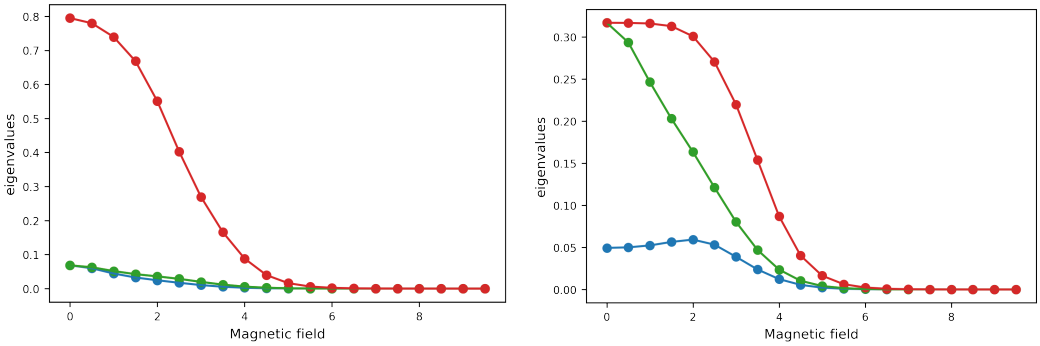

(a) (b)

Figure 4.16: Eigenvalues of the R-Matrix vs. magnetic field for $N = 5$, a: spins (1,2); (b): spins(1,3).

4.2.5 Ten Spins

This section of the thesis aims to investigate the concurrence of the 1D Heisenberg spin chain with a larger number of spins, specifically ten spins on the chain, across high and low temperatures.

In Fig. 4.17, the concurrence for the high-temperature case with $k_BT = 1$ is presented. Consistent with expectations, the concurrence between nearest neighbors is higher than that between next-nearest neighbors. In the absence of a magnetic field, nearest neighbor spins exhibit non-zero concurrence, with the maximum values found at the edges of the chain, i.e., between spins (1,2) and spins (9,10). Conversely, next-nearest neighbors are not entangled. Upon application of a magnetic field, the concurrence between spins (1,2) and spins (9,10) decreases and reaches very small values for $B \geq 6$, while the concurrence between other nearest neighbors on the chain shows peaks and dips before eventually decreasing to values close to zero. Only two pairs of next-nearest neighbor spins, i.e., spins (1,3) and spins (8,10), exhibit non-zero concurrence in the range of non-zero magnetic field.

In Fig. 4.18, we present the concurrence plot for a chain of ten spins at the lower temperature of $k_BT = 0.1$ as a function of magnetic field. Consistent with the high-temperature case shown in Fig. 4.17 for $k_BT = 1$, the nearest neighbor spins exhibit non-zero concurrence, with the maximum values found at the edges of the chain between spins (1,2) and spins (9,10) at zero magnetic field. However, all next-nearest neighbor spins are separable and exhibit zero concurrence in the absence

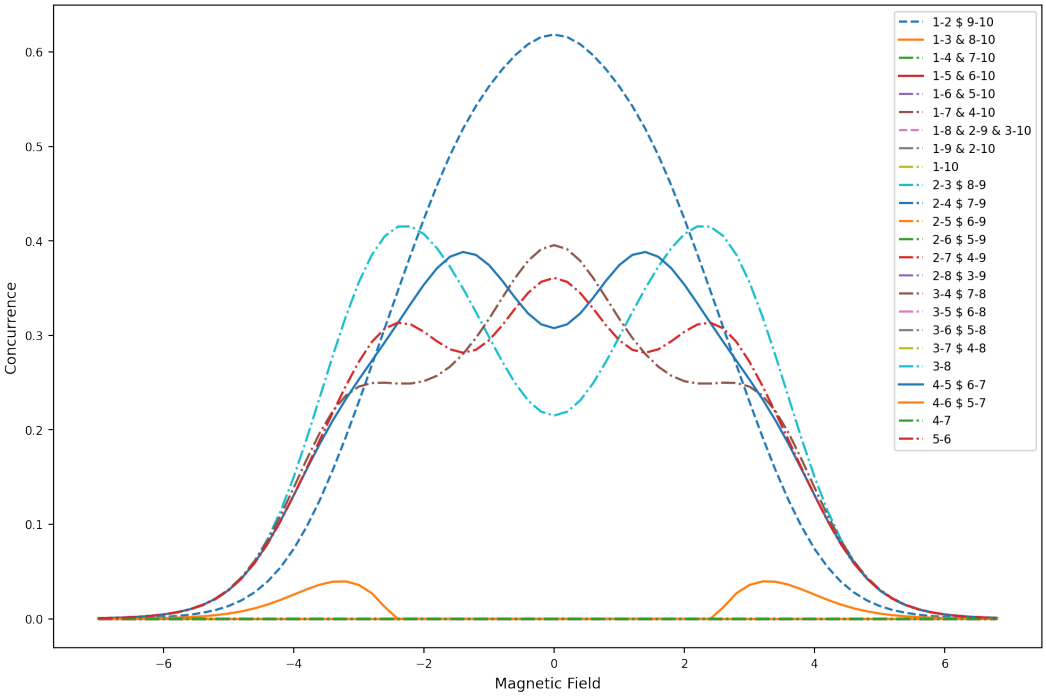

Figure 4.17: Concurrence vs. magnetic field for $N = 10$, $k_BT = 1$, $J = 1$.

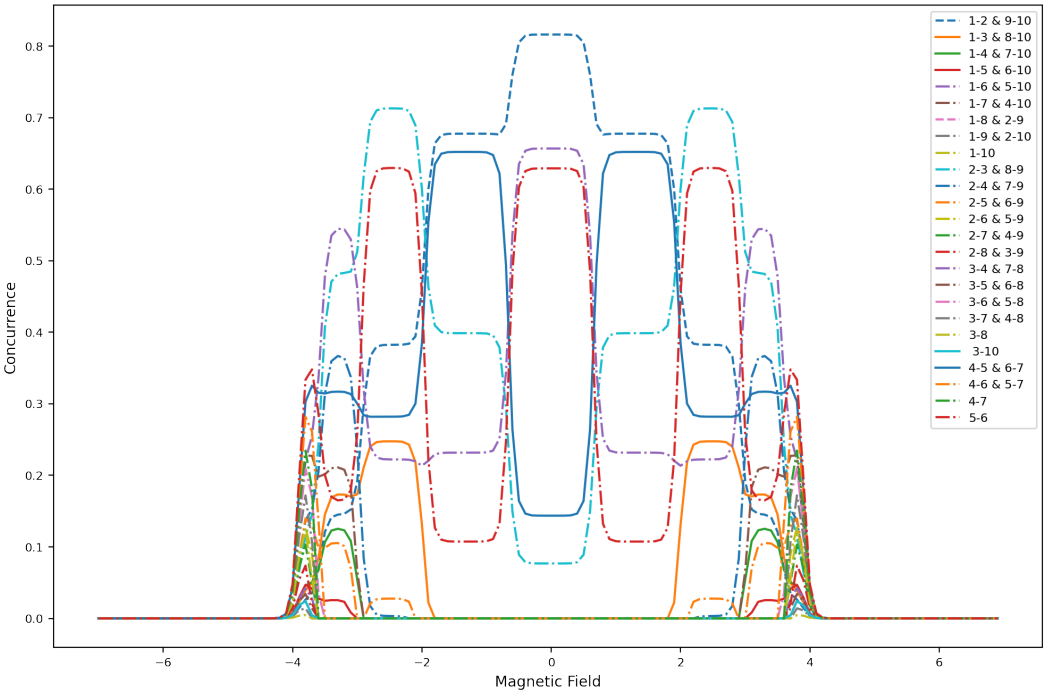

Figure 4.18: Concurrence vs. magnetic field for $N = 10$, $k_BT = 0.1$, $J = 1$.

of a magnetic field. After applying an external magnetic field, the concurrence for nearest neighbors displays maxima and minima before vanishing at around $B \approx 4$. In contrast, the concurrence for next-nearest neighbors is non-zero in the magnetic field range from $B \approx 1.8$ to $B \approx 4$ and vanishes after $B \approx 4$.

In Fig. 4.19, we examine the magnetic field range of $B \approx 1.8$ to $B \approx 4$, where the concurrence exhibits significant changes for low temperature, $k_B T = 0.1$. It is evident from the figure that the concurrence between the first and last spins on the chain, spins (1,10), is minimal and increases with decreasing the number of lattice sites separating the given pairs. Additionally, there are three critical magnetic field ranges in which the concurrence changes notably. In the first two magnetic field ranges, $1.8 < B < 3$ and $3 < B < 3.5$, the concurrence for nearest and next-nearest neighbors displays peaks and dips. However, in the final magnetic field range, $3.5 < B < 4$, the concurrence for pairs of spins with larger numbers of lattice sites between them is non-zero, and a peak in the concurrence for those pairs is observed. Beyond $B \approx 4$, the concurrence for all pairs of spins becomes negligible.

The crossover fields where the concurrence changes significantly correspond to critical points where the entanglement properties of the system undergo a qualitative change. These critical points are determined by the interplay between the strength of the magnetic field and the interactions between the spins. The behavior of the system at these points is physically significant and is related to the existence of quantum phase transitions. Specifically, in our system, the crossover fields mark the boundary between different quantum phases that have distinct entanglement properties. The crossover fields depend on the specific parameters of the system, such as the coupling constants and the temperature, and they may change as one varies these parameters. Similarly, as one changes the number of spins in the system, the entanglement properties of the system may change, leading to different crossover fields.

4.2.6 Entanglement in the Presence of Magnetic Field: Discussion

From our results, it is evident that the symmetry of concurrence for $B \to -B$ and for the antiferromagnetic case $J_x = J_y = J_z = J = 1$ is consistent with Fig. 3(b) in Ref. [19], where the two external magnetic fields are equal. Additionally, in Fig.

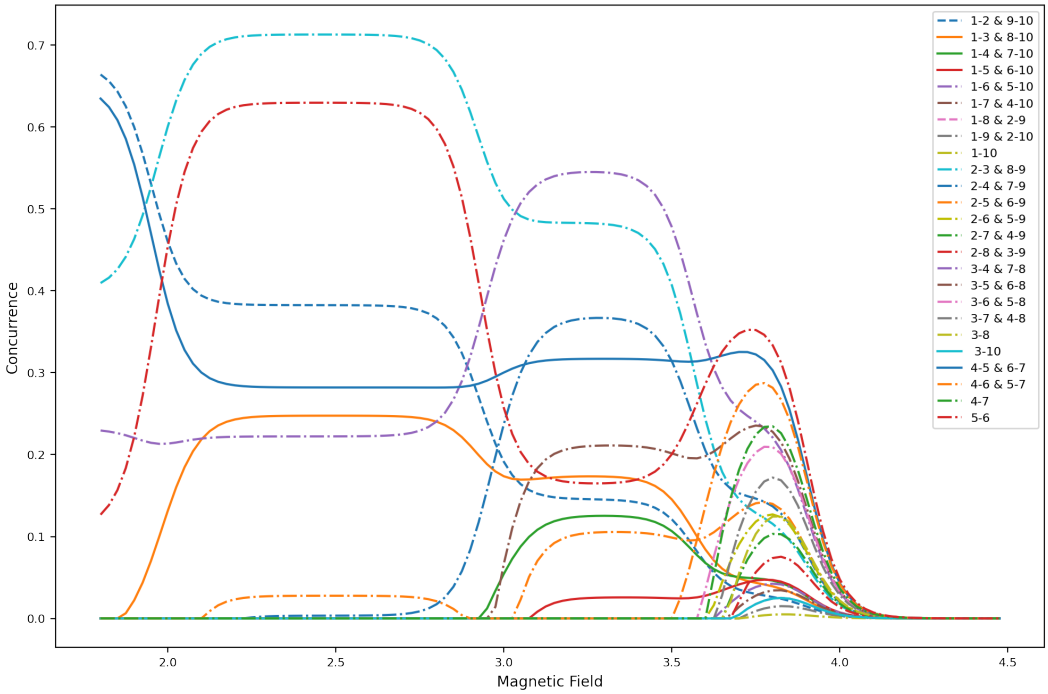

Figure 4.19: Concurrence vs. magnetic field for $N = 10$, $k_BT = 0.1$, $J = 1$. This is a closeup of Fig. 4.18 for $1.8 < B < 4.5$.

4(b) of the Ref. [19], it is shown that by increasing the temperature from $k_BT = 0.9$ to $k_BT = 1.5$, the concurrence vanishes. Our findings are in agreement with this previous work.

Our findings demonstrate that the maximum concurrence between nearest neighbors is larger than the maximum concurrence between next-nearest neighbors in the 1D Heisenberg spin chain. This observation is consistent with the results presented in Fig. 2 of Ref. [18], which specifically examines the case of a six-spin chain for nearest neighbors, next-nearest neighbors, and next-next-nearest neighbors. Our work builds upon these previous findings and provides further insights into the behavior of entanglement in the Heisenberg spin chain. We have extended this analysis to numerous other cases to investigate in more detail the impact of the magnetic field and the number of lattice sites separating given pairs on entanglement. This is an interesting observation that can have important physical consequences in a variety of contexts. For example, in spintronics and quantum computing, the strength of entanglement between neighboring spins can determine the efficiency of quantum gates and the robustness of the quantum state against decoherence.

Furthermore, Refs. [18] confirms the existence of critical ranges of the magnetic field where the concurrence changes significantly, which is in agreement with our results. The critical magnetic field range where the concurrence changes dramatically suggests that there is a phase transition in the system. The exact nature of this phase transition would depend on the specific details of the system, such as the strength of the coupling J and the temperature. Such phase transitions can potentially be important in many-body quantum systems and may have applications in quantum information processing and condensed matter physics.

Furthermore, the lifting of degeneracies by applying an external magnetic field has significant implications for the behavior of the system, including changes in magnetic properties, transport properties, and the emergence of magnetic ordering.

Taken together, these results provide valuable insights into the nature of entanglement in 1D spin systems, and how it is affected by external magnetic fields. In particular, our findings suggest that the entanglement can be used as a sensitive probe of the critical behavior of such systems, and that it can provide valuable information about the underlying symmetries and phase transitions.

Chapter 5

Conclusion and Future works

5.1 Conclusion

Throughout this study, we have investigated the entanglement properties of the one-dimensional Heisenberg spin chain in various scenarios. By utilizing the Hamiltonian of the spin chain, including coupling constants, spin operators, and an external magnetic field in the z-direction, we have derived the density matrix as a function of temperature. Our primary objective was to examine the entanglement between pairs of spins on the chain and explore how it varies with temperature, coupling constants, magnetic field, number of spins, and the number of lattice sites separating given pairs of spins. To accomplish this, we have utilized the concurrence as a measure of entanglement, and the reduced density matrix technique to compute it.

The main results are as follows.

- In general, the behavior of the concurrence with respect to increasing coupling strength depends on the specific values of the coupling constants and the temperature of the system. In the antiferromagnetic case with all positive coupling constants, the concurrence generally increases with increasing coupling strength. However, in other cases, such as in the presence of a magnetic field or in the presence of different signs or magnitudes of coupling constants, the concurrence can exhibit more complex behavior, such as non-monotonic behavior or decreasing behavior with increasing coupling strength.

- The entanglement decreases as temperature increases and converges to small values or vanishes in the high-temperature limit. The high-temperature limit refers to the limit at which the thermal energy is much greater than the energy scale of the interactions between the spins. In this limit, the entanglement between the spins is greatly reduced. The high-temperature limit depends on the other parameters of the problem, such as the number of spins and the coupling constants, which can affect the energy scale of the interactions and the stability of the magnetic ordering in the system. Therefore, the specific values of the high-temperature limit can vary for different parameter values.

- The relation between entanglement and an external magnetic field in the z-direction is not as straightforward as the relation between entanglement and temperature or coupling constants. The critical range of the magnetic field in the z-direction significantly affects the entanglement in the system, and its specific values depend on factors such as the number of spins, temperature, and coupling constants. This range can indicate the presence of a phase transition and can exhibit non-monotonic or oscillatory behavior in the concurrence.

- Another exciting result of this work is the entanglement of a pair of spins versus the number of lattice sites separating given pairs(i.e., pairs of spins for which we are studying the entanglement). Generally, the entanglement decreases as the number of lattice sites separating given pairs increases.

Furthermore, our research has potential applications in quantum information processing and quantum computing. Entanglement is a key resource in quantum communication and computing, and our study provides a better understanding of how it can be generated and manipulated in one-dimensional Heisenberg spin chains. Additionally, our results can be used to design more efficient and accurate quantum algorithms and simulations that rely on entanglement in spin chains.

5.2 Future works

Some possible extensions of this research are as follows.

- For future investigations, it would be valuable to determine the extent of entanglement for a large number of spins, beyond the ten spins on the chain considered

in this study, to comprehend how the entanglement varies for different pairs of spins. However, this endeavor is highly challenging and computationally expensive due to the dimension of the Hamiltonian and density matrix, which is $2^N * 2^N$ for N spins on the chain. To perform such calculations, it is necessary to utilize compiler languages such as C++ and Fortran, which are not as straightforward as Python for modeling entanglement. This future work is essential to gain a better understanding of the nature of entanglement in many-body systems, and it could have significant implications for the development of quantum computing and other quantum technologies.

- Another promising avenue for future work is to explore the effects of anisotropic external magnetic fields on the entanglement properties of spin systems. By applying spatially varying magnetic fields in different directions, we can study how the entanglement changes between different pairs of spins and gain insights into the anisotropic nature of entanglement in these systems. Such investigations could have significant implications for the development of spin-based quantum devices and technologies, making this an exciting area for future research.

- For future work, it is also interesting to perform a more thorough study of the entanglement in spin chains under the combined effect of magnetic fields, coupling constants, and temperature. To achieve this, it is necessary to plot 3D graphs of the concurrence and study their relationship with these variables. Such an analysis can provide new insights into the behavior of entanglement in spin systems and its dependence on different physical parameters, leading to potential applications in quantum technologies.

Appendix A

Mathematical operations for quantifying entanglement

This appendix includes illustrative examples of fundamental mathematical tools used in the context of quantum information, such as natural logarithms, exponentials, square roots, and the partial transpose of matrices. Additionally, an example of the Peres-Horodecki criterion is provided in the following section. Finally, the mathematical description of the Bell Inequality is presented for reference. First, we consider a matrix like this:

$$A = \begin{pmatrix} 6 & -4 \\ 3 & -1 \end{pmatrix}.$$

The eigenvalues and eigenvectors of this matrix are:

$$\lambda_1 = 3, \lambda_2 = 2, V_1 = (4, 3), V_2 = (1, 1).$$

Now, we can generate the matrix and the inverse matrix based on the eigenvectors and the eigenvalues of matrix A.

By utilizing equation (2.1), we are able to calculate the natural logarithm of matrix A.

$$\log A = \begin{pmatrix} 4 & 1 \\ 3 & 1 \end{pmatrix} \begin{pmatrix} \ln 3 & 0 \\ 0 & \ln 2 \end{pmatrix} \begin{pmatrix} 1 & -1 \\ -3 & 4 \end{pmatrix},$$

$$\log A = \begin{pmatrix} \ln\left(\frac{81}{8}\right) & 4\ln\left(\frac{2}{3}\right) \\ 3\ln\left(\frac{3}{2}\right) & \ln\left(\frac{16}{9}\right) \end{pmatrix}.$$

The method to find the square root and the exponential of a matrix is the same, the only difference is that we have to replace the square root and the exponential of the eigenvalues of matrix A on the main diagonal elements. Equation (2.2) enables us to determine the exponential of matrix A.

$$\exp A = \begin{pmatrix} 4 & 1 \\ 3 & 1 \end{pmatrix} \begin{pmatrix} \exp 3 & 0 \\ 0 & \exp 2 \end{pmatrix} \begin{pmatrix} 1 & -1 \\ -3 & 4 \end{pmatrix},$$

$$\exp A = \begin{pmatrix} 58.2 & -50.8 \\ 38.1 & -30.7 \end{pmatrix}.$$

And finally, for the square root of the matrix A, we have:

$$\sqrt{A} = \begin{pmatrix} 4 & 1 \\ 3 & 1 \end{pmatrix} \begin{pmatrix} \sqrt{3} & 0 \\ 0 & \sqrt{2} \end{pmatrix} \begin{pmatrix} 1 & -1 \\ -3 & 4 \end{pmatrix},$$

$$\sqrt{A} = \begin{pmatrix} 2.7 & -1.3 \\ 0.9 & 0.5 \end{pmatrix}.$$

This method to find the natural logarithm, square root, and exponential of a matrix works for any dimensionality of a diagonalizable square matrix, provided the eigenvalues are greater than or equal to zero.

In this section, we study an example of the Peres–Horodecki criterion. As an example, we consider the density for the two-qubit Werner's states,

$$\rho = p|\psi^-\rangle\langle\psi^-| + (1-p)\frac{I}{4}.$$

Where $0 \leq p \leq 1$, I is the identity matrix , and $|\psi^- >= \frac{1}{\sqrt{2}}(|+-\rangle - |-+\rangle)$. Now, we can write the density matrix:

$$|\psi^-\rangle\langle\psi^-| = \frac{1}{2}(|+-\rangle\langle+-| - |+-\rangle\langle-+| + |-+\rangle\langle-+| - |-+\rangle\langle+-|).$$

Can be written as the matrix:

$$= \frac{1}{4}\begin{pmatrix} 0 & 0 & 0 & 0 \\ 0 & 2 & -2 & 0 \\ 0 & -2 & 2 & 0 \\ 0 & 0 & 0 & 0 \end{pmatrix},$$

and

$$\frac{I}{4} = \frac{1}{4}\begin{pmatrix} 1 & 0 & 0 & 0 \\ 0 & 1 & 0 & 0 \\ 0 & 0 & 1 & 0 \\ 0 & 0 & 0 & 1 \end{pmatrix},$$

this gives us

$$\rho = \frac{1}{4}\begin{pmatrix} 1-p & 0 & 0 & 0 \\ 0 & p+1 & -2p & 0 \\ 0 & -2p & p+1 & 0 \\ 0 & 0 & 0 & 1-p \end{pmatrix}.$$

From section 2.3.4, we know that the positive partial transpose of a matrix can be calculated from equation (2.14). We can find the partial transpose of the density matrix as ρ^T:

$$\rho^T = \frac{1}{4}\begin{pmatrix} 1-p & 0 & 0 & -2p \\ 0 & p+1 & 0p & 0 \\ 0 & 0 & p+1 & 0 \\ -2p & 0 & 0 & 1-p \end{pmatrix}.$$

In our analysis, we utilized the Peres-Horodecki criterion, which establishes that if all eigenvalues of the positive partial transpose of the density matrix are positive, the system is separable. Conversely, if at least one eigenvalue is negative, the system is entangled. In our example, the eigenvalues were calculated to be $\lambda_{1,2,3} = \frac{1+p}{4}$ and $\lambda_4 = \frac{1-3p}{4}$. Our calculations showed that the eigenvalue λ_4 is negative for the range $1 \geq p > \frac{1}{3}$, indicating that the state is entangled within this range. This finding highlights the significance of the Peres-Horodecki criterion as a tool for identifying entangled states.

In this section, I follow the derivation given in Ref. [5]. Let us consider two spins $\frac{1}{2}$ particles, labeled as A and B, which are entangled and in a singlet state. The singlet

state is given by:

$$|\psi\rangle = \frac{1}{\sqrt{2}}(|\uparrow_A\rangle \otimes |\downarrow_B\rangle - |\downarrow_A\rangle \otimes |\uparrow_B\rangle), \tag{A.1}$$

where $|\uparrow_A\rangle$ and $|\downarrow_A\rangle$ are the spin-up and spin-down states of particle A, respectively, and $|\uparrow_B\rangle$ and $|\downarrow_B\rangle$ are the spin-up and spin-down states of particle B, respectively. Now, let us define two observables for each particle, labeled as A_0 and A_1 for particle A, and B_0 and B_1 for particle B. Each observable has two possible outcomes, +1 or -1, corresponding to the spin-up or spin-down state. If we consider the following combination, if they are hidden variables

$$\langle A_0B_0\rangle + \langle A_0B_1\rangle + \langle A_1B_0\rangle + \langle A_1B_1\rangle = \tag{A.2}$$

$$a_0b_0 + a_0b_1 + a_1b_0 - a_1b_1 = (a_0 + a_1)b_0 + (a_0 - a_1)b_1 \leq 2,$$

where a_0 and a_1 correspond to the possible values that can be obtained when measuring the properties represented by A_0 and A_1, respectively, and b_0 and b_1 correspond to the possible values that can be obtained when measuring the properties represented by B_0 and B_1, respectively. Since a_0 and a_1 can only take the values of $+1$ or -1, it follows that $a_0 = a_1$ or $a_0 = -a_1$. When a_0 and a_1 have the same value, the term $(a_0 - a_1)b_1$ becomes zero, while when a_0 and a_1 have opposite values, the term $(a_0 + a_1)b_0$ becomes zero. Therefore, one of the terms on the right-hand side of the Bell inequality expression will vanish, and the other will either equal $+2$ or -2.

In the example we are considering, A_0 and A_1 represent measurements of spin in the z and x directions, respectively, and B_0 and B_1 represent measurements of spin in the directions of $-(\hat{x}+\hat{z})/\sqrt{2}$ and $(\hat{x}-\hat{z})/\sqrt{2}$, respectively, with multipied by $\frac{2}{\hbar}$. We will now utilize the singlet state given in equation A.1 and evaluate the combination given in equation A.2 to analyze the Bell inequality.

$$\begin{aligned}
\langle\psi|A_0B_0|\psi\rangle &= \frac{4}{\hbar^2}\frac{1}{2}\left[(\langle\uparrow\downarrow| - \langle\downarrow\uparrow|)(S_{1z})\frac{(-S_{2z} - S_{2x})}{\sqrt{2}}(|\uparrow\downarrow\rangle + |\downarrow\uparrow\rangle)\right] \\
&= \frac{4}{\hbar^2}\frac{\hbar^2}{4}\frac{1}{2\sqrt{2}}(\langle\uparrow\downarrow|\uparrow\downarrow\rangle + \langle\downarrow\uparrow|\downarrow\uparrow\rangle) = \frac{1}{\sqrt{2}}, \\
\langle\psi|A_0B_1|\psi\rangle &= \frac{4}{\hbar^2}\frac{1}{2}\left[(\langle\uparrow\downarrow| - \langle\downarrow\uparrow|)(S_{1z})\frac{(S_{2x} - S_{2z})}{\sqrt{2}}(|\uparrow\downarrow\rangle + |\downarrow\uparrow\rangle)\right] = \frac{1}{\sqrt{2}},
\end{aligned}$$

$$\langle\psi|A_1B_0|\psi\rangle = \frac{4}{\hbar^2}\frac{1}{2}\left[(\langle\uparrow\downarrow| - \langle\downarrow\uparrow|)(S_{1x})\frac{(-S_{2x} - S_{2z})}{\sqrt{2}}(|\uparrow\downarrow\rangle + |\downarrow\uparrow\rangle)\right] = \frac{1}{\sqrt{2}},$$

$$\langle\psi|A_1B_1|\psi\rangle = \frac{4}{\hbar^2}\frac{1}{2}\left[(\langle\uparrow\downarrow| - \langle\downarrow\uparrow|)(S_{1x})\frac{(S_{2x} - S_{2z})}{\sqrt{2}}(|\uparrow\downarrow\rangle + |\downarrow\uparrow\rangle)\right] = -\frac{1}{\sqrt{2}},$$

then, we can write:

$$\langle A_0B_0\rangle + \langle A_0B_1\rangle + \langle A_1B_0\rangle - \langle A_1B_1\rangle = 2\sqrt{2}.$$

The violation of the inequality $\langle A_0B_0\rangle + \langle A_0B_1\rangle + \langle A_1B_0\rangle - \langle A_1B_1\rangle \leq 2$, which was derived from the assumption of local hidden variables, indicates the failure of local realism and confirms the success of the Bell inequality.

Appendix B

Python codes

This section outlines the key functions used to calculate the Hamiltonian, density matrix, and concurrence in our work. Specifically, the following Python function is employed to obtain the Hamiltonian of the 1D Heisenberg spin chain.

```
def ham(N, J, B):
    sx_ls =  []
    sy_ls =  []
    sz_ls =  []
    sz_ls2 =  []
    for i in range(N):
        if(i < 2):
            sx_ls.append(sigmax())
            sy_ls.append(sigmay())
            sz_ls.append(sigmaz())
        else:
            sx_ls.append(identity(2))
            sy_ls.append(identity(2))
            sz_ls.append(identity(2))

    for i in range(N):
        if(i < 1):
```

```
            sz_ls2.append(sigmaz())
        else:

            sz_ls2.append(identity(2))

    summ = 0

    for k in range(N-1):
        summ = summ
        + J[0] * tensor(make_obj(np.roll(sx_ls, k, axis=0)))
        + J[1] * tensor( make_obj( np.roll(sy_ls, k, axis=0)))
        + J[2] * tensor(make_obj( np.roll(sz_ls, k, axis=0)))
    for k in range(N):
        summ = summ - B * tensor(make_obj( np.roll(sz_ls2, k, axis=0)))
    return summ
```

The Python function used to compute the Hamiltonian of the 1D Heisenberg spin chain takes three inputs: N for the number of spins, J for the list of three values for the coupling constants, and B for the magnetic field. The np.roll function in NumPy is used to shift the spin operators and identity matrices in the Hamiltonian function. The first for loop generates the spin operators, which are Pauli matrices in the normalized case, and the two-by-two identity matrices. The second for loop generates the z component of the Pauli matrices for the external magnetic field part in the Hamiltonian. Once we obtain the Hamiltonian matrix, we require another function to compute the density matrix.

```
def density_maker(H, T):
    Exp_H = (-H/T).expm()

    P_func = Exp_H.tr()

    Density_Matrix = (Exp_H)/(P_func)
```

```
    return Density_Matrix
```

In our code, the function to find the density matrix takes two inputs, the Hamiltonian matrix H and the temperature T. To obtain the reduced density matrix for each pair of spins, we utilize the ptrace function available in QuTiP. Finally, we have a function to compute the concurrence between each pair of spins, completing the necessary steps to analyze the entanglement in the Heisenberg spin chain.

```
def concurrence(rho):
    sysy = tensor(sigmay(), sigmay())

    rho_tilde = (sysy * rho.conj()) * sysy

    R_Matrix = (rho.sqrtm() * rho_tilde) * rho.sqrtm()
    R_Matrix2 = R_Matrix.sqrtm()

    evals = R_Matrix2.eigenenergies()

    evals = np.sort(np.real(evals))

    lsum = (evals[3]) - (evals[2]) - (evals[1]) - (evals[0])

    return max(0, lsum)
```

This function takes the reduced density matrix of each pair of spins as input. The R-matrix and its eigenvalues are calculated inside this function to obtain the concurrence.

Bibliography

[1] Ryszard Horodecki, Paweł Horodecki, Michał Horodecki, and Karol Horodecki. Quantum entanglement. *Reviews of Modern Physics*, 81(2):865–942, 2009.

[2] Vlatko Vedral. Recent advances in quantum information theory reveal the deep connections between entanglement and thermodynamics, many-body theory, quantum computing and its link to macroscopicity. *Nature Physics*, 10:4, 2014.

[3] Karol Życzkowski, Paweł Horodecki, Michał Horodecki, and Ryszard Horodecki. Dynamics of quantum entanglement. *Physical Review A*, 65:012101, 2001.

[4] Barbara M. Terhal. Detecting quantum entanglement. *Theoretical Computer Science*, 287, 2002.

[5] Michael A. Nielsen and Isaac L. Chuang. *Quantum computation and quantum information*. Cambridge University Press, 10th anniversary edition, 2010.

[6] Michael Levin and Xiao-Gang Wen. Detecting topological order in a ground state wave function. *Physical review letters*, 96(11):110405, 2006.

[7] M Zahid Hasan and Charles L Kane. Colloquium: topological insulators. *Reviews of modern physics*, 82(4):3045, 2010.

[8] Jason Alicea. New directions in the pursuit of majorana fermions in solid state systems. *Reports on progress in physics*, 75(7):076501, 2012.

[9] A. Einstein, B. Podolsky, and N. Rosen. Can quantum-mechanical description of physical reality be considered complete? *Physical Review*, 47:777–780, 1935.

[10] N. Bohr. Can quantum-mechanical description of physical reality be considered complete? *Physical Review*, 48:696–702, 1935.

[11] J. S. Bell. On the Einstein Podolsky Rosen paradox. *Physics Physique Fizika*, 1:195–200, Nov 1964.

[12] John S. Bell. *Speakable and Unspeakable in Quantum Mechanics*. Cambridge University Press. p. 65, 1987.

[13] John B. Parkinson and Damian J. J. Farnell. *An Introduction to Quantum Spin Systems*. Springer/Sci-Tech/Trade; 2010th edition, 2010.

[14] J I Latorre and A Riera. A short review on entanglement in quantum spin systems. *Journal of Physics A: Mathematical and Theoretical*, 42(50):504002, 2009.

[15] V. Vedral, M. B. Plenio, M. A. Rippin, and P. L. Knight. Quantifying entanglement. *Physical Review Letters*, 78:2275–2279, 1997.

[16] Christopher Eltschka and Jens Siewert. Quantifying entanglement resources. *Journal of Physics A: Mathematical and Theoretical*, 47(42), 2014.

[17] Xiaoguang Wang. Entanglement in the quantum Heisenberg XY model. *Physical Review A*, 64:012313, 2001.

[18] M. C. Arnesen, S. Bose, and V. Vedral. Natural thermal and magnetic entanglement in the 1D Heisenberg model. *Physical Review Letters*, 87:017901, 2001.

[19] Yang Sun, Yuguang Chen, and Hong Chen. Thermal entanglement in the two-qubit Heisenberg XY model under a nonuniform external magnetic field. *Phys. Rev. A*, 68:044301, Oct 2003.

[20] Guo-Feng Zhang and Shu-Shen Li. Thermal entanglement in a two-qubit Heisenberg XXZ spin chain under an inhomogeneous magnetic field. *Physical Review A*, 72(3):034302, 2005.

[21] H.A. Zad. Entanglement in the mixed-three-spin XXX Heisenberg model with the next-nearest-neighbour interaction. *Acta Physica Polonica B*, 46(10):1911, 2015.

[22] Min Cao and Shiqun Zhu. Thermal entanglement between alternate qubits of a four-qubit Heisenberg XX chain in a magnetic field. *Physical Review A*, 71(3):034311, 2005.

[23] Awad H. Al-Mohy and Nicholas J. Higham. Improved inverse scaling and squaring algorithms for the matrix logarithm. *SIAM Journal on Scientific Computing*, 34(4):C153–C169, 2012.

[24] Rajendra Bhatia. *Matrix Analysis*, volume 169 of *Graduate Texts in Mathematics*. Springer New York, 1997.

[25] Khakim D. Ikramov. Hamiltonian square roots of skew-hamiltonian matrices revisited. *Linear Algebra and its Applications*, 325(1):101–107, 2001.

[26] G. Vidal, J. I. Latorre, E. Rico, and A. Kitaev. Entanglement in quantum critical phenomena. *Physical Review Letters*, 90(22), 2003.

[27] Subir Sachdev. *Quantum Phase Transitions*. Cambridge University Press, 2nd edition, 2011.

[28] Tobias J. Osborne and Michael A. Nielsen. Entanglement in a simple quantum phase transition. *Physical Review A*, 66(3):032110, 2002.

[29] Gustavo Rigolin. Thermal entanglement in the two-qubit Heisenberg XYZ model. *International Journal of Quantum Information*, 2(03):393–405, 2004.

[30] U. Fano. Description of states in quantum mechanics by density matrix and operator techniques. *Reviews of Modern Physics*, 29:74–93, 1957.

[31] A.S. Holevo. *Statistical Structure of Quantum Theory*. Lecture Notes in Physics Monographs. Springer, 2001.

[32] P. A. M. Dirac. Note on exchange phenomena in the Thomas atom. *Mathematical Proceedings of the Cambridge Philosophical Society*, 26(3), 1930.

[33] J. Eisert, M. Cramer, and M. B. Plenio. Colloquium: Area laws for the entanglement entropy. *Reviews of Modern Physics*, 82:277–306, 2010.

[34] Pasquale Calabrese and John Cardy. Entanglement entropy and quantum field theory. *Journal of Statistical Mechanics: Theory and Experiment*, 2004(06):P06002, 2004.

[35] Asher Peres. Separability criterion for density matrices. *Physical Review Letters*, 77:1413–1415, 1996.

[36] Michał Horodecki, Paweł Horodecki, and Ryszard Horodecki. Mixed-state entanglement and distillation: Is there a "bound" entanglement in nature? *Physical Review Letters*, 80:5239–5242, 1998.

[37] William Wootters. Entanglement of formation and concurrence. *Quantum Information & Computation*, 1:27–44, 2001.

[38] Scott Hill and William K. Wootters. Entanglement of a pair of quantum bits. *Physical Review Letters*, 78(26):5022–5025, 1997.

[39] William K Wootters. Entanglement of formation of an arbitrary state of two qubits. *Physical Review Letters*, 80(10):2245, 1998.

[40] Lan Zhou and Yu-Bo Sheng. Concurrence measurement for the two-qubit optical and atomic states. *Entropy*, 17(6):4293–4322, 2015.

[41] M. B. Plenio. Logarithmic negativity: A full entanglement monotone that is not convex. *Physical Review Letters*, 95:090503, 2005.

[42] Charles R. Harris, K. Jarrod Millman, Stéfan J. van der Walt, Ralf Gommers, Pauli Virtanen, David Cournapeau, Eric Wieser, Julian Taylor, Sebastian Berg, Nathaniel J. Smith, Robert Kern, Matti Picus, Stephan Hoyer, Marten H. van Kerkwijk, Matthew Brett, Allan Haldane, Jaime Fernández del Río, Mark Wiebe, Pearu Peterson, Pierre Gérard-Marchant, Kevin Sheppard, Tyler Reddy, Warren Weckesser, Hameer Abbasi, Christoph Gohlke, and Travis E. Oliphant. Array programming with NumPy. *Nature*, 585(7825):357–362, 2020.

[43] J. D. Hunter. Matplotlib: A 2D graphics environment. *Computing in Science & Engineering*, 9(3):90–95, 2007.

[44] J.R. Johansson, P.D. Nation, and Franco Nori. QuTiP: An open-source python framework for the dynamics of open quantum systems. *Computer Physics Communications*, 183(8):1760–1772, 2012.

[45] J.R. Johansson, P.D. Nation, and Franco Nori. QuTiP 2: A python framework for the dynamics of open quantum systems. *Computer Physics Communications*, 184(4):1234–1240, 2013.

[46] Shi-Jian Gu, Haibin Li, You-Quan Li, and Hai-Qing Lin. Entanglement of the Heisenberg chain with the next-nearest-neighbor interaction. *Phys. Rev. A*, 70:052302, Nov 2004.

[47] Xiaoguang Wang. Threshold temperature for pairwise and many-particle thermal entanglement in the isotropic Heisenberg model. *Phys. Rev. A*, 66:044305, Oct 2002.

[48] L. Campos Venuti, C. Degli Esposti Boschi, and M. Roncaglia. Long-distance entanglement in spin systems. *Phys. Rev. Lett.*, 96:247206, Jun 2006.

[49] Xiaoguang Wang. Thermal and ground-state entanglement in Heisenberg XX qubit rings. *Phys. Rev. A*, 66:034302, Sep 2002.